A&A 464, 581–599 (2007)
DOI: 10.1051/0004-6361:20054396

Astronomy & Astrophysics

A brown dwarf desert for intermediate mass stars in Scorpius OB2?⋆,⋆⋆

M. B. N. Kouwenhoven[1,⋆⋆⋆], A. G. A. Brown[2], and L. Kaper[1]

[1] Astronomical Institute "Anton Pannekoek", University of Amsterdam, Kruislaan 403, 1098 SJ Amsterdam, The Netherlands
e-mail: t.kouwenhoven@sheffield.ac.uk; [kouwenho;lexk]@science.uva.nl
[2] Leiden Observatory, University of Leiden, PO Box 9513, 2300 RA Leiden, The Netherlands
e-mail: brown@strw.leidenuniv.nl

Received 21 October 2005 / Accepted 21 November 2006

ABSTRACT

We present JHK_S observations of 22 intermediate-mass stars in the Scorpius-Centaurus OB association, obtained with the NAOS/CONICA system at the ESO Very Large Telescope. This survey was performed to determine the status of (sub)stellar candidate companions of Sco OB2 member stars of spectral type A and late-B. The distinction between companions and background stars is made on the basis of a comparison to isochrones and additional statistical arguments. We are sensitive to companions with an angular separation of 0.1″−11″ (13−1430 AU) and the detection limit is K_S = 17 mag. We detect 62 stellar components of which 18 turn out to be physical companions, 11 candidate companions, and 33 background stars. Three of the 18 confirmed companions were previously undocumented as such. The companion masses are in the range 0.03 $M_\odot \leq M \leq$ 1.19 $M_\odot$, corresponding to mass ratios $0.06 \leq q \leq 0.55$. We include in our sample a subset of 9 targets with multi-color ADONIS observations from Kouwenhoven et al. (2005, A&A, 430, 137). In the ADONIS survey secondaries with $K_S < 12$ mag were classified as companions; those with $K_S > 12$ mag as background stars. The multi-color analysis in this paper demonstrates that the simple $K_S = 12$ mag criterion correctly classifies the secondaries in ∼80% of the cases. We reanalyse the total sample (i.e. NAOS/CONICA and ADONIS) and conclude that of the 176 secondaries, 25 are physical companions, 55 are candidate companions, and 96 are background stars. Although we are sensitive (and complete) to brown dwarf companions as faint as K_S = 14 mag in the semi-major axis range 130−520 AU, we detect only one, corresponding to a brown dwarf companion fraction of 0.5 ± 0.5% ($M \gtrsim 30\ M_J$). However, the number of brown dwarfs is consistent with an extrapolation of the (stellar) companion mass distribution into the brown dwarf regime. This indicates that the physical mechanism for the formation of brown dwarf companions around intermediate mass stars is similar to that of stellar companions, and that the embryo ejection mechanism does not need to be invoked in order to explain the small number of brown dwarf companions among intermediate mass stars in the Sco OB2 association.

Key words. binaries: visual – binaries: general – stars: formation – stars: low mass, brown dwarfs – open clusters and associations: individual: Sco OB2

1. Introduction

The predominance of star formation in binary or multiple systems inside stellar clusters makes the binarity and multiplicity of newly born stars one of the most sensitive probes of the process of star and star cluster formation (see Blaauw 1991, and references therein). Ideally one would like to have detailed knowledge of the binary population at the time that the stars are being formed. However, this is difficult to achieve in practice and therefore we have embarked on a project to characterize the observationally better accessible "primordial binary population", which is defined as *the population of binaries as established just after the gas has been removed from the forming system, i.e., when the stars can no longer accrete gas from their surroundings* (Kouwenhoven et al. 2005). We chose to focus our efforts on the accurate characterization of the binary population in nearby OB associations. The youth and low stellar density of OB associations ensure that their binary population is very similar to the primordial binary population. We refer to Kouwenhoven et al. (2005) and Kouwenhoven (2006) for a more extensive discussion and motivation of this project.

Our initial efforts are concentrated on the Sco OB2 association. Sco OB2 consists of the three subgroups Upper Scorpius (US), Upper Centaurus Lupus (UCL), and Lower Centaurus Crux (LCC). The properties of the subgroups are listed in Table 1. Its stellar population is accurately known down to late A-stars thanks to the *Hipparcos* catalogue (de Zeeuw et al. 1999), and extensive literature data is available on its binary population (Brown 2001). In addition Sco OB2 has recently been the target of an adaptive optics survey of its *Hipparcos* B-star members (Shatsky & Tokovinin 2002). We have conducted our own adaptive optics survey of 199 A-type and late-B type stars in this association (Kouwenhoven et al. 2005) using the ADONIS instrument, which was mounted on the ESO 3.6 meter telescope at La Silla, Chile. We performed these observations in the K_S-band (and for a subset of the targets additionally in the J and H band). We detected 151 stellar components other than the target stars and used a simple brightness criterion to separate background stars[1] from physical companions. All components fainter than

⋆ Based on observations collected at the European Southern Observatory, Chile. Program 073.D-0354(A).

⋆⋆ Appendix A is only available in electronic form at http://www.aanda.org

⋆⋆⋆ *Current address*: Department of Physics and Astronomy, Hicks Building, Hounsfield Road, Sheffield S3 7RH, UK.

[1] When mentioning "background star", we refer to any stellar object that does not belong to the system, including foreground stars.

Table 1. Multiplicity among *Hipparcos* members of the three subgroups of Sco OB2. The columns show the subgroup name (Upper Scorpius; Upper Centaurus Lupus; Lower Centaurus Crux), the distance (see de Zeeuw et al. 1999), the age (de Geus et al. 1989; Preibisch et al. 2002 for US; Mamajek et al. 2002 for UCL and LCC), the number of known single stars, binary stars, triple systems and $N > 3$ systems, and the binary statistics (see Sect. 7), after inclusion of the new results presented in this paper.

	D (pc)	Age (Myr)	S	B	T	>3	$F_{\rm M}$	$F_{\rm NS}$	$F_{\rm C}$
US	145	5–6	64	44	8	3	0.46	0.67	0.61
UCL	140	15–22	132	65	19	4	0.40	0.61	0.52
LCC	118	17–23	112	57	9	1	0.37	0.56	0.44
all			308	166	36	8	0.41	0.61	0.51

$K_{\rm S}$ = 12 mag were considered background stars; all brighter components were identified as candidate companion stars (see also Shatsky & Tokovinin 2002). Of the 74 candidate physical companions 33 were known already and 41 were new candidate companions.

In examining the binary properties of our sample of A and late B-stars we noticed that at small angular separations (≤4 arcsec) no companions fainter than $K_{\rm S} \approx 12$ mag are present, assuming that the sources fainter than $K_{\rm S} \approx 14$ mag are background stars (as we had no information on their colors). The absence of companions with $K_{\rm S} > 12$ mag and $\rho < 4''$ is clearly visible in Fig. 3 of Kouwenhoven et al. (2005). This result implies that A and B stars do not have close companions with masses less than about 0.08 $M_{\odot}$, unless the assumed background stars *are* physical companions. In the latter case the close faint sources would be brown dwarfs (which are known to be present in Sco OB2; see Martín et al. 2004) and a gap would exist in the companion mass distribution. In either case a peculiar feature would be present in the mass distribution of companions which has to be explained by the binary formation history.

We decided to carry out follow-up multi-color observations in order (1) to determine the reliability of our $K_{\rm S}$ = 12 mag criterion to separate companions and background stars, (2) to investigate the potential gap or lower limit of the companion mass distribution, and (3) to search for additional close and/or faint companions.

These follow-up near-infrared observations were conducted with NAOS/CONICA (NACO) on the ESO Very Large Telescope at Paranal, Chile. We obtained $JHK_{\rm S}$ photometric observations of 22 A and late-B members in Sco OB2 and their secondaries[2]. In Sect. 2 we describe our NACO sample, the observations, the data reduction procedures, and photometric accuracy of the observations. In Sect. 3 we describe the detection limit and completeness limit of the ADONIS and NACO observations. In Sect. 4 we determine the status (companion or background star) of the secondaries with multi-color observations. We perform the analysis for the secondaries around the 22 NACO targets, and for those around the 9 targets in the ADONIS sample for which we have multi-color observations. In Sect. 4 we also analyze the background star statistics, and we evaluate the accuracy of the $K_{\rm S}$ = 12 mag separation criterion. In Sect. 5 we derive for each companion its mass and mass ratio. In Sect. 6 we discuss the lack of brown dwarf companions with separations between 1″ and 4″ (130−520 AU) in our sample, and discuss whether or not the brown dwarf desert exists for A and late-B type members of Sco OB2. Finally, we present updated binary statistics of the Sco OB2 association in Sect. 7 and summarize our results in Sect. 8.

[2] We use the term "secondary" for any stellar component in the field near the target star. A secondary can be a companion star or a background star.

Table 2. We have obtained follow-up multi-color observations with NACO for 22 targets in the Sco OB2 association. We include in our analysis 9 targets with multi-color observations in the ADONIS sample. All targets listed above are known to have secondaries in the ADONIS survey. The table lists for each star the parallax and error (taken from de Bruijne 1999), the $K_{\rm S}$ magnitude, and the spectral type of the primary star. The $K_{\rm S}$ magnitudes are those derived in this paper for the 22 stars observed with NACO, and are taken from Kouwenhoven et al. (2005) for the other nine stars. The last column shows the subgroup membership of each star (US = Upper Scorpius; UCL = Upper Centaurus Lupus; LCC = Lower Centaurus Crux), taken from de Zeeuw et al. (1999).

HIP #	HD #	π (mas)	σ_π (mas)	$K_{\rm S}$ (mag)	Type	Group
NAOS/CONICA targets						
59502	106036	10.26	0.49	6.87	A2V	LCC
60851	108501	9.63	0.50	6.06	A0Vn	LCC
61265	109197	7.50	0.48	7.46	A2V	LCC
62026	110461	9.20	0.45	6.31	B9V	LCC
63204	112381	9.07	0.49	6.78	A0p	LCC
67260	119884	8.15	0.49	6.98	A0V	LCC
67919	121040	9.64	0.49	6.59	A9V	LCC
68532	122259	8.09	0.43	7.02	A3 IV/V	UCL
69113	123445	5.92	0.41	6.37	B9 V	UCL
73937	133652	8.17	0.46	6.23	Ap Si	UCL
78968	144586	5.87	0.53	7.42	B9 V	US
79098	144844	7.28	0.45	5.69	B9 V	US
79410	145554	7.00	0.52	7.09	B9 V	US
79739	146285	6.79	0.52	7.08	B8 V	US
79771	146331	6.86	0.51	7.10	B9 V	US
80142	147001	5.82	0.44	6.66	B7 V	UCL
80474	147932	7.20	0.51	5.80	B5 V	US
80799	148562	7.91	0.52	7.45	A2 V	US
80896	148716	7.77	0.57	7.44	F3 V	US
81949	150645	6.21	0.52	7.33	A3 V	UCL
81972	150742	5.36	0.40	5.87	B3 V	UCL
83542	154117	5.00	0.53	5.38	G8/K0 III	US
ADONIS multi-color subset						
53701	95324	7.93	0.58	6.48	B8 IV	LCC
76071	138343	5.96	0.56	7.06	B9 V	US
77911	142315	6.87	0.49	6.68	B9 V	US
78530	143567	7.11	0.48	6.87	B9 V	US
78809	144175	7.20	0.51	7.51	B9 V	US
78956	144569	5.55	0.50	7.57	B9.5 V	US
79124	144925	6.41	0.53	7.13	A0 V	US
79156	144981	6.21	0.53	7.61	A0 V	US
80238	147432	7.64	0.68	7.34	A1 III/IV	US

2. Observations and data reduction

2.1. Definition of the NACO sample

The major goals of our NACO follow-up observations are to determine the validity of the $K_{\rm S}$ = 12 mag criterion that we used to separate companions and background stars in our ADONIS sample (Kouwenhoven et al. 2005), to study the companion mass distribution near the stellar-substellar boundary, and to search for additional faint and/or close companions.

Our NACO sample consists of 22 member stars (listed in Table 2) in the Sco OB2 association: 10 of spectral type B, 10 of spectral type A, and one each of spectral type F and G.

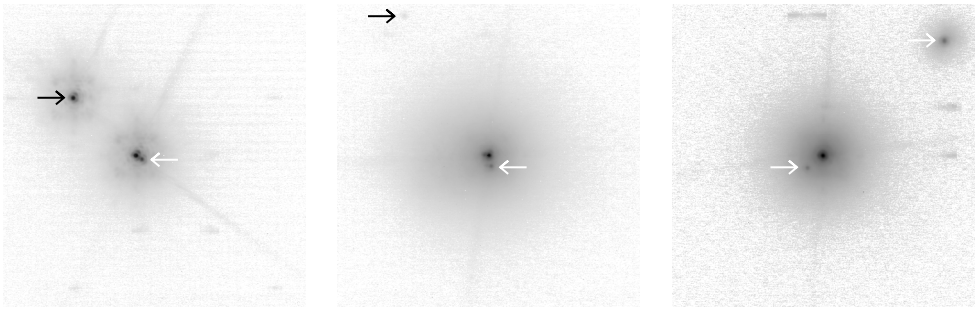

Fig. 1. With our NACO survey we find three close companions (shown in the figure), which were not detected in our ADONIS survey. The panels ($6.6'' \times 6.6''$) are centered on the primary stars. *Left:* the binary HIP 63204 in K_S, with a companion at angular separation $0.15''$ and a background star at angular separation $1.87''$. *Middle:* the binary HIP 73937 in K_S, with a close companion at $\rho = 0.24''$ and a background star at $\rho = 3.56''$. *Right:* HIP 79771 in K_S, with two companion stars at $\rho = 0.44''$ and $\rho = 3.67''$. Companions are indicated with white arrows and background stars with black arrows. Several artifacts are visible in the fields of HIP 63204 and HIP 79771, which can easily be recognized as such. The panels show a subset of the total field of view for each observation, which is $14'' \times 14''$. For these three targets we observe no stellar components other than those shown in the panels.

The targets are more or less equally distributed over the three subgroups of Sco OB2: 9 in US, 6 in UCL, and 7 in LCC. All 22 targets are known to have secondaries in the ADONIS survey.

We included in our sample all seven target stars with faint ($K_S > 14$ mag) and close ($\leq$4 arcsec) candidate background stars: HIP 61265, HIP 67260, HIP 73937, HIP 78968, HIP 79098, HIP 79410, and HIP 81949. The other 15 targets all have candidate companion stars, for which we will use the multi-color data to further study their nature. Priority was given to target stars with multiple secondaries (candidate companions and candidate background stars) and targets close to the Galactic plane (HIP 59502, HIP 60851, HIP 80142, and HIP 81972) because of the larger probability of finding background stars.

There are 9 targets in the ADONIS dataset with (photometric) multi-color observations. These targets are also listed in Table 2 and all have secondaries. Kouwenhoven et al. (2005) use only the K_S magnitude to determine the status of a secondary, including the secondaries around the 9 targets with J_S observations. Later, in Sect. 4, we will combine the data of the 22 NACO targets and the 9 ADONIS targets with multi-color observations, and determine the status of the secondaries of these 31 targets using their JHK_S magnitudes. In the remaining part of Sect. 2 we describe the NACO observations, data reduction procedures, and photometric accuracy.

2.2. NACO observations

The observations were performed using the NAOS/CONICA system, consisting of the near-infrared camera CONICA (Lenzen et al. 1998) and the adaptive optics system NAOS (Rousset et al. 2000). NAOS/CONICA is installed at the Nasmyth B focus of UT4 at the ESO Very Large Telescope on Paranal, Chile. The observations were carried out in Service Mode on the nights of April 6, April 28–30, May 4–5, June 8, June 19, June 25, June 27–28, July 3, July 24, and September 10, 2004. Some representative images are shown in Fig. 1.

The targets were imaged using the S13 camera, which has a pixel scale of 13.27 mas/pixel, and a field of view of $14'' \times 14''$. The CONICA detector was an Alladin 2 array in the period April 6 to May 5, 2004. The detector was replaced by an Alladin 3 array in May 2004, which was used for the remaining observations. We used the readout mode Double_RdRstRd and the detector mode HighDynamic. For both detectors, the rms readout noise was 46.2 e^- and the gain was $\approx$11 e^-/ADU. The full-well capacity of the Alladin 2 array is 4300 ADU, with a linearity limit at about 50% of this value. For the Alladin 3 array the full-well capacity is 15 000 ADU, with the linearity limit at about two-thirds of this value.

Each observation block corresponding to a science target includes six observations. The object is observed with the three broad band filters J (1.253 μm), H (1.643 μm), and K_S (2.154 μm). Since our targets are bright, several of them will saturate the detector, even with the shortest detector integration time. For this reason we also obtained measurements in J, H, and K_S with the short-wavelength neutral density filter (hereafter NDF). The NDF transmissivity is about 1.4% in the near-infrared. The observations *with* NDF allow us to study the primary star and to obtain an accurate point spread function (PSF), while the observations *without* NDF allow us to analyze the faint companions in detail. In order to characterize the attenuation of the NDF we observed the standard stars GSPC S273-E and GSPC S708-D. These are LCO/Palomar NICMOS Photometric Standards (Persson et al. 1998). The near-infrared magnitudes of these stars are consistent with spectral types G8V and G1V, respectively. By comparing the detected JHK_S fluxes, with and without the NDF, we determined the attenuation of the NDF in the three filters.

Each observation consisted of six sequential exposures of the form $OSSOOS$, where O is the object, and S is a sky observation. Each exposure was jittered using a jitter box of 4 arcsec. We used a sky offset of 15 arcsec, and selected a position angle such that no object was in the sky field.

Each exposure consists of 5 to 35 short observations of integration times in the range 0.35−5.3 s, depending on the brightness of the source. For the target observations without NDF we chose the minimum integration time of 0.35 s. For all standard star observations and target observations with NDF we chose the integration time such that the image does not saturate for reasonable Strehl ratios. We optimized the integration time to obtain the desired signal-to-noise ratio. The short integrations are combined by taking the median value.

Visual wavefront sensing was performed directly on the target stars, which minimized the effects of anisoplanatism. For a subset of the target stars, the observation block was carried out multiple times. The target stars were usually positioned in the center of the field. Occasionally we observed the target off-center to be able to image a companion at large angular separation.

The observations on the nights of 29 April, 28 June, and 3 July, 2004, were obtained under bad weather or instrumental conditions and were removed from the dataset. These observations were repeated under better conditions later on in the observing run. The observations on the nights of 6 April and 27 June, 2004, were partially obtained under non-photometric conditions, and were calibrated using the targets themselves (see Sect. 2.5). All other observations were performed under photometric conditions. Most observations (85%) were obtained with a seeing between 0.5 and 1.5 arcsec. For a large fraction of the remaining observations the seeing was between 1.5 and 2.0 arcsec. The majority (65%) of the observations were obtained at an airmass of less than 1.2, and for 98% of the observations the airmass was less than 1.6.

2.3. Data reduction procedures

The primary data reduction was performed with the ECLIPSE package (Devillard 1997). Calibration observations, including dark images, flat field images, and standard star images, were provided by ESO Paranal. Twilight flat fields were used to create a pixel sensitivity map. For several observations, no twilight flats were available. In these cases we used the lamp flats. The dark-subtracted observations were flatfielded and sky-subtracted. Finally, the three jittered object observations were combined.

2.4. Component detection

The component detection is performed with the STARFINDER package (Diolaiti et al. 2000). The PSF of the target star is extracted from the background subtracted image. The flux of the primary star is the total flux of the extracted PSF. A scaled-down version of the PSF is compared to the other signals in the field with a peak flux larger than 2.5−3 times the background noise[3]. The profile of these signals is then cross-correlated with the PSF. Only those signals with a profile very similar to that of the PSF star (i.e., a correlation coefficient larger than ≈0.7) are considered as real detections. Finally, the angular separation, the position angle, and the flux of the detected component are derived.

As discussed in Sect. 2.2, we observe each target in JHK_S *with* NDF to obtain an accurate PSF template, and *without* NDF to do accurate photometry on the faint companions. The observations without NDF are often saturated, which makes PSF extraction impossible. None of the observations with NDF are saturated. Since these observations are carried out close in time and close in airmass, we assume that the PSFs of the observations with and without NDF are not significantly different. This is illustrated in Fig. 2, where we plot the radial profiles of the extracted PSF of HIP 78968. For the saturated images we use the PSF that was extracted from the corresponding non-saturated image for analysis of the secondaries.

Artifacts are present in the image when observing a bright object. The location of the artifacts is well-defined (CONICA manual), and since the artifacts look significantly non-circular, they can be easily recognized as non-stellar components (see Fig. 1). Additionally, observations obtained with the NDF show a faint artifact at ∼2 arcsec to the North-East of the target star. Care was taken that the extracted PSF and the analysis of companions in that area were not affected by the presence of this artifact.

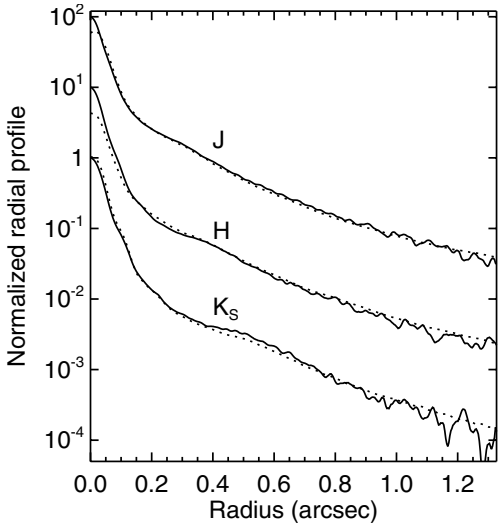

Fig. 2. The radial profile of the PSF for the target star HIP 78968. The observations are obtained using the NACO system in the night of May 5, 2004 in J, H, and K_S. The corresponding Strehl ratios for these observations are 6.5% in J, 15.6% in H, and 23.6% in K_S. Observations are obtained with neutral density filter (NDF; solid curves) and without NDF (dotted curves). The profiles are normalized such that the peak flux for the images obtained with NDF is 100 in J, 10 in H, and 1 in K_S. The observations with NDF allow us to extract the PSF and measure the flux of the primary star. The images obtained without NDF are much deeper, but the primary is usually saturated. Assuming the PSF is similar, we use the non-saturated PSF to analyze the secondaries in the saturated image.

2.5. Photometry

Observations of standard stars from the Persson et al. (1998) catalog were provided by ESO. The standard stars are used to determine the magnitude zeropoints for each night and each filter individually. No standard stars are available in the nights of 28 April and 10 September, 2004. For 28 April we determine the zero point magnitude using 2MASS as a reference system, and the target stars HIP 67260, HIP 67919, HIP 68532 as substitute standard stars. For 10 September, we use the 2MASS data for HIP 83542 to calibrate J and H. For the K_S filter we use the HIP 83542 measurement of Kouwenhoven et al. (2005) since its 2MASS K_S magnitude is inaccurate due to confusion with the diffraction spike of a nearby star. The H magnitude of HIP 59502 was obtained under non-photometric conditions on 6 April, 2004, so instead we used the corresponding 2MASS measurement of this star. All observations in the night of 27 June, 2004 were obtained under non-photometric conditions; the fluxes of HIP 80474 and HIP 81972 are therefore calibrated using 2MASS. We derive the calibrated magnitudes using the mean extinction coefficients for Paranal: $k_J = 0.11$, $k_H = 0.06$, and $k_{K_S} = 0.07$.

The attenuation $m_{\rm NDF}$ (in magnitudes) of the NDF is determined for J, H, and K_S using the standard stars GSPC S273-E and GSPC S708-D and the non-saturated target stars. All observations are performed in pairs (with and without NDF), which allows us to determine the NDF attenuation. For each filter $m_{\rm NDF}$ is calculated as the median difference in magnitude: $m_{\rm NDF} = \langle m_{\star,\text{without NDF}} - m_{\star,\text{with NDF}} \rangle$. We find $m_{{\rm NDF},J} = 4.66 \pm 0.03$ mag, $m_{{\rm NDF},H} = 4.75 \pm 0.02$ mag, and $m_{{\rm NDF},K_S} = 4.85 \pm 0.02$ mag,

[3] Note that a peak flux of 2.5−3 times the background noise corresponds to a total flux with a much larger significance, since the flux of a faint companion is spread out over many pixels. All detected components in our survey have a signal-to-noise ratio larger than 12.8.

respectively. We do not measure a significant difference between the values found for the early-type program stars and the late-type standard stars. All observations done with the NDF are corrected with the values mentioned above.

2.6. Photometric precision and accuracy of the NACO observations

We estimate the photometric uncertainty of the NACO observations using simulations (see Sect. 2.6.1) and the comparison with other datasets (Sects. 2.6.2–2.6.4). For primaries, the external 1σ error in J, H, and K_S is ∼0.04 mag, corresponding to an error of ∼0.06 mag in the colors. Typical 1σ external errors in magnitude and color for the bright companions ($8 \lesssim K_S/\mathrm{mag} \lesssim 13$) are 0.08 mag and 0.11 mag, respectively. For the faintest sources ($K_S \gtrsim 13$ mag) the errors are 0.12 mag in magnitude and 0.17 mag in color. In the following subsections we will discuss the analysis of our photometric errors.

2.6.1. Algorithm precision

The instrumental magnitudes of all objects are obtained using STARFINDER. We investigate the precision of the STARFINDER algorithm using simulated observations. We create simulations of single and binary systems with varying primary flux (10^4–10^6 counts), flux ratio (ΔK_S = 0–10 mag), angular separation (0″–13″), Strehl ratio (1%–50%), and position angle. We estimate the flux error by comparing the input flux with the flux measured by STARFINDER for several realizations.

Using the simulations we find that the precision of the STARFINDER fluxes is ∼1% (∼0.01 mag) for most primary stars in our sample, for all relevant Strehl ratios and as long as the PSF of the primary star is not significantly influenced by the presence of a companion. The 1% error is due to the tendency of STARFINDER to over-estimate the background underneath bright objects (Diolaiti et al. 2000). For the fainter primaries in our sample (flux between 5×10^4 and 5×10^5 counts), the flux error is 1–3% (∼0.01–0.03 mag).

For secondaries outside the PSF-halo of the primary, the error is typically ∼0.01 mag if the flux difference with the primary is less than 5 mag. Fainter secondaries have a larger flux error, ranging from 0.01 mag to 0.1 mag, depending on the brightness of primary and companion.

If the secondary is in the halo of the primary, its flux error is somewhat larger. For example, for a companion at $\rho = 2''$ which is less than 4 mag fainter than the primary, the flux error is 4% (∼0.04 mag) or smaller. Deblending the PSF of a primary and close secondary does not introduce a much larger error, as long as the magnitude difference is less than ∼5 mag. No close companions with a magnitude difference larger than 5 mag are detected in our NACO observations.

For several fields the observations without NDF are saturated. In order to analyze the faint companions in the field we use the PSF of the corresponding non-saturated observation obtained with the NDF (see Sect. 2.2). These observations are performed close in airmass and time, so that their PSFs are similar. We estimate the flux error by comparing PSFs corresponding to non-saturated images obtained with NDF and without NDF. These comparisons show that the resulting error ranges from 0.02 to 0.5 mag, depending on the brightness of the secondary. We therefore minimize flux calculations using this method, and only use measurements obtained with the PSF of the non-saturated image when no other measurements are available. In the latter case, we place a remark in Table A.1.

2.6.2. Comparison with 2MASS

We compare the near-infrared measurements of the 22 targets in our NACO survey with the measurements in 2MASS (Cutri et al. 2003) to get an estimate of the external errors. We only select those measurements in 2MASS that are not flagged. Since the resolution in our observations is higher than the ≈4″ resolution of 2MASS, we combine the observed fluxes of the primaries and close companions before the comparison with 2MASS. For the observations *not* calibrated with the 2MASS measurements, the rms difference between our measurements and those of 2MASS are 0.055 mag in J, 0.040 mag in H, and 0.049 mag in K_S.

2.6.3. Comparison with the ADONIS survey of Kouwenhoven et al. (2005)

We detect all but two of the stellar components found by Kouwenhoven et al. (2005) around the 22 target stars in our NACO survey. We do not observe the faint companions of HIP 80142 at $\rho = 8.54''$ and HIP 81949 at $\rho = 9.70''$ because they are not within our NACO field of view. We find three bright companions at small angular separation of HIP 63204 ($\rho = 0.15''$), HIP 73937 ($\rho = 0.34''$), and HIP 79771 ($\rho = 0.44''$). Since these objects are not found in the ADONIS observations of Kouwenhoven et al. (2005), their fluxes and those of the corresponding primaries are summed for comparison with Kouwenhoven et al. (2005).

The rms difference between the 22 primaries observed with NACO and those described in Kouwenhoven et al. (2005) is 0.055 mag in K_S. HIP 69113 and HIP 78968 additionally have multi-color observations in Kouwenhoven et al. (2005), which are in good agreement with the measurements presented in this paper. The J and H measurements of HIP 80474 and HIP 80799 are flagged "non-photometric" in Kouwenhoven et al. (2005), and are not discussed here.

Our dataset and that of Kouwenhoven et al. (2005) have 35 stellar components other than the target stars in common. The rms difference between the K_S magnitude of these objects in the two papers is 0.26 mag. The differences are similar for the objects that have common J and H measurements in both papers.

2.6.4. Comparison with Shatsky & Tokovinin (2002)

Three targets in our NACO survey are also included in the binarity survey amongst B-stars in Sco OB2 by Shatsky & Tokovinin (2002): HIP 79098, HIP 80142, and HIP 81972. Seven secondaries are detected both their survey and in our NACO survey (1 for HIP 79098; 2 for HIP 80142; 4 for HIP 81972). Shatsky & Tokovinin (2002) classify these seven secondaries all as "definitely optical" or "likely optical". They performed their observations in both coronographic and non-coronographic mode, and were therefore able to find five faint secondaries which do not appear in our NACO sample.

The J and K_S magnitudes of HIP 79098 and HIP 80142 and their companions are in good agreement with our measurements. Our measurements of HIP 81972 are in good agreement with those in 2MASS as well as the measurements in Kouwenhoven et al. (2005), but there is a discrepancy between our measurements of HIP 81972 and those in Shatsky & Tokovinin (2002). The magnitude difference between HIP 81972 and its

companions in our observations and in Shatsky & Tokovinin (2002) are similar. The observations of HIP 81972 are flagged "likely photometric" in Shatsky & Tokovinin (2002), but since they disagree with those in this paper and those in 2MASS, we assume they are non-photometric, and ignore them for the magnitude comparison.

2.7. General properties of the NACO observations

In the fields around the 22 targets we observed with NACO, we find 62 components other than the target stars. The properties of these targets and their secondaries are listed in Table A.1. The 22 primaries have 5.5 mag $< J <$ 7.8 mag, 5.0 mag $< H <$ 7.7 mag, and 4.9 mag $< K_S <$ 7.7 mag. The brightest companions observed are ~7.5 mag in the three filters, while the faintest secondaries found have J = 16.6 mag, H = 17.3 mag, and K_S = 17.3 mag.

With NACO we detect components in the angular separation range $0.15'' < \rho < 11.8''$. The lower limit on ρ depends on the Strehl ratio and the magnitude difference between primary and companion (see also Sect. 3). The upper limit is determined by the size of the field-of-view. The median formal error in angular separation is 4 mas for bright components (8 mag $\lesssim K_S \lesssim$ 13 mag) and 10 mas for faint components ($K_S \gtrsim$ 13 mag). Position angles are measured from North to East. The median formal error in the position angle is 0.°007.

We find 27 stellar components that are not detected by Kouwenhoven et al. (2005). Three close secondaries are found at small angular separation from HIP 63204-2 (ρ = 0.15″; K_S = 8.40 mag), HIP 73937-1 (ρ = 0.34″; K_S = 8.37 mag), and HIP 79771-2 (ρ = 0.44″; K_S = 11.42 mag). The former two have been reported as candidate companions (Worley & Douglass 1997); the latter was previously undocumented. The other 25 new secondaries are all faint ($K_S \gtrsim$ 12 mag). Two of these 25 secondaries were also reported by Shatsky & Tokovinin (2002).

3. The completeness and detection limit of the ADONIS and NACO surveys

We cannot detect sources fainter than a certain magnitude because of the background noise in the images. The faintest detectable magnitude additionally depends on the angular distance to the primary star, the primary star magnitude, and the Strehl ratio. For a correct interpretation of the results of the survey it is therefore important to characterize the limiting magnitude of the observations (the detection limit) and the magnitude at which a star is likely detected (the completeness limit).

We study the completeness limit and detection limit as a function of angular separation from the primary for six stars. These are HIP 58859, HIP 65178, and HIP 76048 from our ADONIS survey and HIP 80799, HIP 78968, and HIP 81949 from our NACO survey. These stars are selected to cover the range in Strehl ratio of the observations, so that the completeness and detection limits are representative for the other targets in the ADONIS and NACO surveys.

For each observation STARFINDER extracts the PSF from the image (see Sect. 2.4). We simulate observations by artificially adding a scaled and shifted copy of the PSF to the observed image. We reduce the simulated image as if it were a real observation. We repeat this procedure twenty times for simulated secondaries with different angular separation and magnitude. We define the detection limit and completeness limit as the magnitude (as a function of angular separation) at which respectively 50% and 90% of the simulated secondaries are detected. The curves in Fig. 3 show the completeness and detection limit for the six stars mentioned above. Due to our sampling the magnitude error of the completeness and detection limit is ~0.15 mag. The figure clearly shows that a high Strehl ratio facilitates the detection of closer and fainter objects as compared to observations with lower Strehl ratio. For all stars the completeness limit is ~0.3 mag above the detection limit.

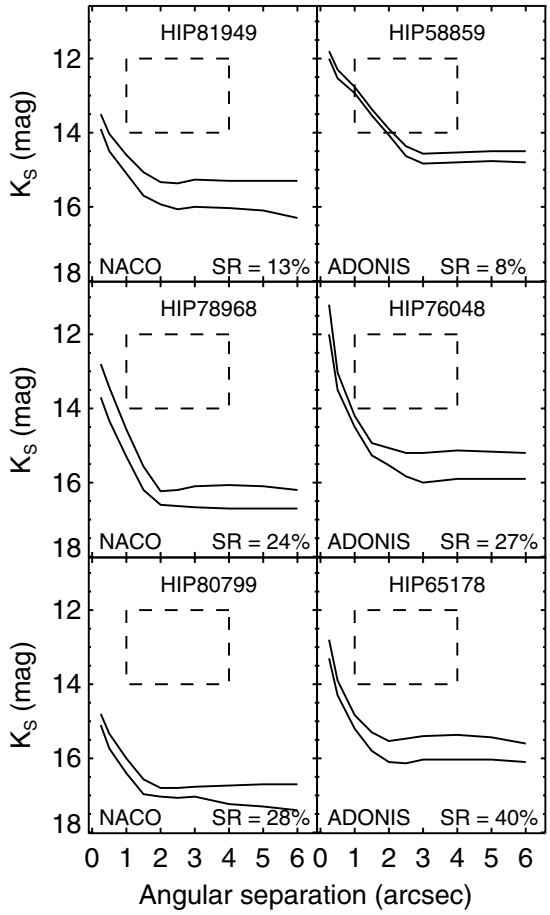

Fig. 3. The detection limit and completeness limit for several targets in our ADONIS survey (Kouwenhoven et al. 2005) and NACO survey (this paper). The target star, Strehl ratio, and instrument are indicated in each panel. The lower and upper curve show the detection limit and the completeness limit, respectively. The detection and completeness limits shown above are representative for the ADONIS and NACO observations. The target stars have K_S magnitudes of 7.33 mag (HIP 81949), 7.42 mag (HIP 78968), 7.45 mag (HIP 80799), 6.52 mag (HIP 58859), 6.26 mag (HIP 76048), and 6.71 mag (HIP 65178). The completeness limit is generally ~0.3 mag brighter than the detection limit. At close angular separation a higher Strehl ratio results in a fainter detection limit. The dashed rectangle encloses the region with 12 mag $\leq K_S \leq$ 14 mag and $1'' \leq \rho \leq 4''$, which is relevant for our analysis of the substellar population in Sco OB2 (see Sect. 6). In this region the NACO observations are complete and ADONIS observations are more than 95% complete.

In Sect. 6 we analyze the substellar companion population in Sco OB2 in the angular separation range $1'' \leq \rho \leq 4''$ and magnitude range 12 mag $\leq K_S \leq$ 14 mag. The NACO observations of 22 targets are complete in this region. Only a few targets in the ADONIS sample are incomplete in this region. Assuming a flat semi-major axis distribution, we estimate that about 5% of the faint companions at small angular separation

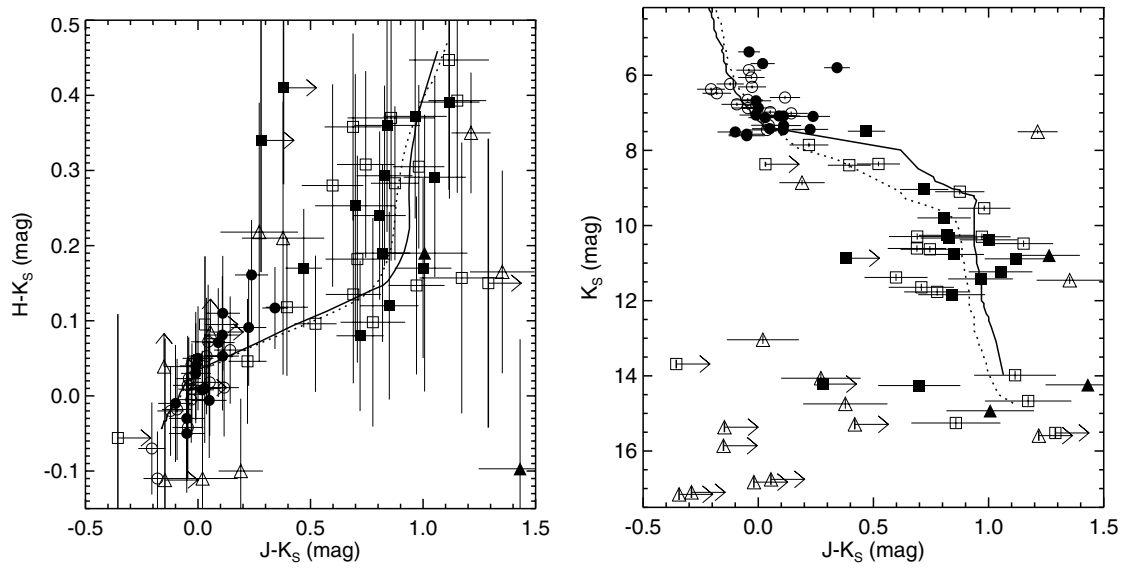

Fig. 4. The color–color diagram (*left*) and color–magnitude diagram (*right*) of the objects in our sample. Measurements are shown for the 22 targets observed with NACO and for the 9 targets with multi-color observations in the ADONIS sample. Both panels show target stars (circles), confirmed and candidate companions (squares), and background stars (triangles). The target stars and secondaries in the US subgroup are indicated with filled symbols; those from UCL and LCC are indicated with open symbols. The 1σ error bars are indicated for all data points. Lower limits are given for objects that are not detected in all three filters. Several detected objects are outside the ranges of the figures; these are all background stars. The status (companion or background star) of the secondaries is discussed in Sect. 4.2. The 5 Myr isochrone for US and the 20 Myr isochrone for UCL and LCC are indicated with the solid and dotted curves, respectively.

are undetected for the 177 targets that are *only* observed with ADONIS (see Fig. 3). For the combined NACO and ADONIS sample this means that we are more than 95% complete in the region 12 mag $\leq K_S \leq$ 14 mag and $1'' \leq \rho \leq 4''$.

With NACO we are sensitive down to brown dwarfs and massive planets. To estimate the mass corresponding to the faintest detectable magnitude as a function of angular separation, we use the models of Chabrier et al. (2000). We assume a distance of 130 pc, the mean distance of Sco OB2, and an age of 5 Myr for the US subgroup and 20 Myr for the UCL and LCC subgroups (cf. Sect. 4.1). At a distance of 130 pc, the brightest brown dwarfs have an apparent magnitude of $K_S \approx 12$ mag. With NACO we are able to detect brown dwarfs at an angular separation larger than $\approx 0.3''$. The magnitude of the faintest detectable brown dwarf increases with increasing angular separation between $\rho = 0.3''-2''$. The minimum detectable mass is a function of age due to the cooling of the brown dwarfs. For angular separations larger than $\approx 2''$ the halo of the primary PSF plays a minor role. For these angular separations we are sensitive (but not complete) down to $K_S \approx 16.5$ mag with NACO, corresponding to planetary masses possibly as low as $\sim 5\ M_J$ for US and $\sim 10\ M_J$ for UCL and LCC. However, because of the large number of background stars and the uncertain location of the isochrone for young brown dwarfs and planets, we will not attempt to identify planetary companions in this paper (see Sect. 4.2 for a further discussion).

Several secondaries are not detected in one or two filters. For the filter(s) in which the secondary is not observed we determine a lower limit on the magnitude of the missing star using simulations. We perform the simulations as described in Kouwenhoven et al. (2005). The position of the secondary is known from observations in other filters. This position is assigned to the simulated companion, so that the detection limit as a function of angular separation is taken into account. Images are created with simulated secondaries of different magnitude. We reduce the images as if they were real observations. The lower limit on the magnitude is then determined by the faintest detectable simulated secondary. Two secondaries (HIP 73937-1 and HIP 76071-1) have a lower limit in J because they are unresolved in the wings of the primary star PSF. The other secondaries with a lower magnitude limit for a filter have a flux below the background noise.

4. Status of the stellar components

In this section we determine the status (companion star or background star) of the secondaries. We analyze the secondaries detected around the 22 targets observed with NACO, as well as the secondaries around the 9 targets with multi-color observations in the ADONIS sample. For the 31 targets analyzed in this section we detect 72 secondaries in total. Sco OB2 members and their companions should be located near the isochrone in the color–magnitude diagram, while the background stars should show a much larger spread. We use this property in Sect. 4.2 to separate companions and background stars. As a consistency check we study in Sect. 4.3 how our results compare to the expected number of background stars in our observations.

4.1. Color–magnitude diagram and isochrones

For the 22 targets in the NACO sample and the 9 targets in the ADONIS multi-color subset we have magnitudes in three filters, as well as for most of their secondaries. Several of the faintest secondaries are undetected in one or two filters, as they are below the detection limit. Color–color and color–magnitude diagrams with the 31 targets and 72 secondaries are shown in Fig. 4. Lower limits are indicated for objects that are not detected in all three filters. Several secondaries in our sample are either very red or very blue. These secondaries fall outside the plots in Fig. 4, and are all background stars.

For our analysis we adopt the isochrones described in Kouwenhoven et al. (2005), which consist of models from

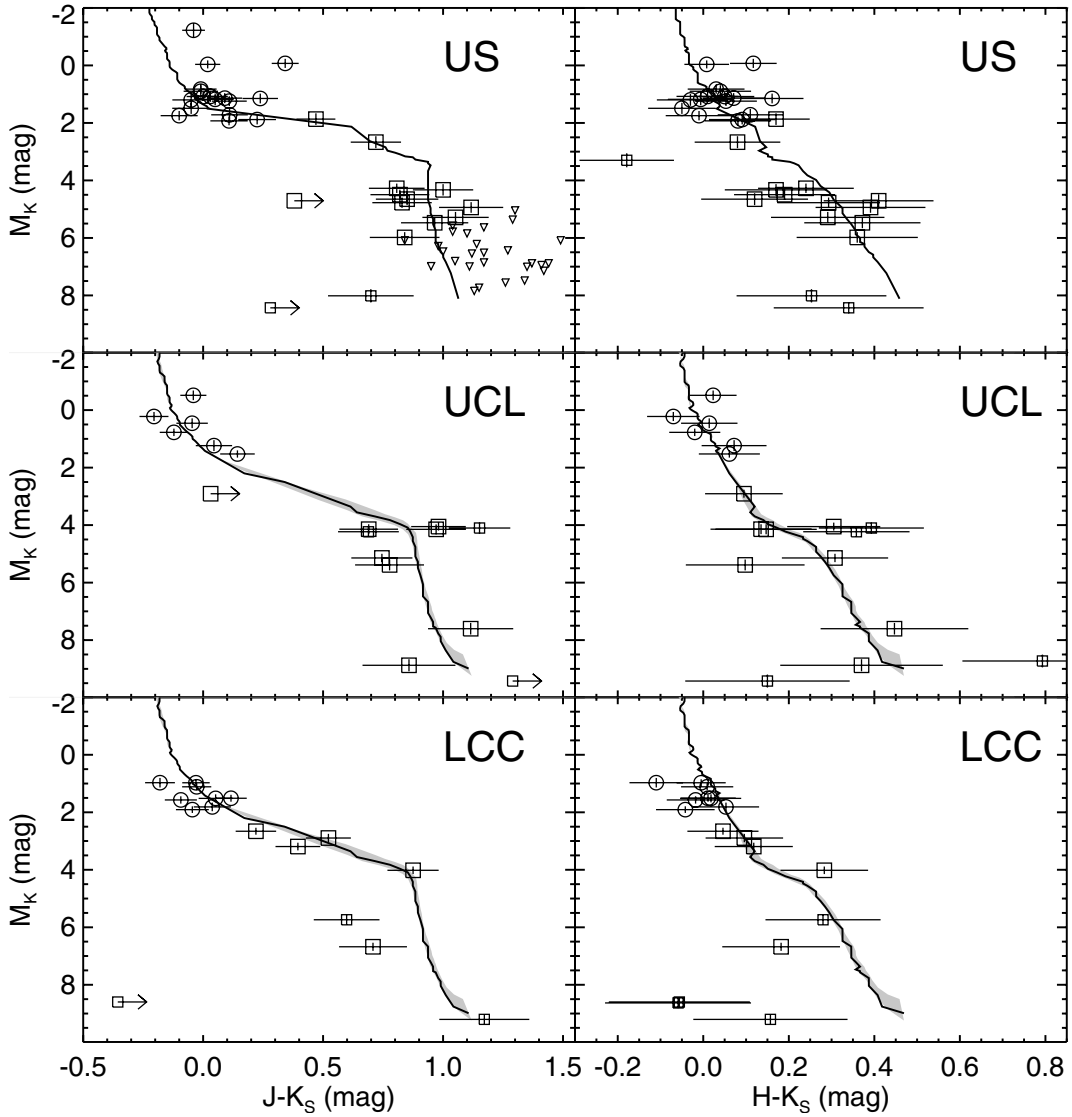

Fig. 5. The (absolute) color–magnitude diagrams for the 22 targets in our NACO sample and the 9 targets with multi-color observations in the ADONIS sample. The results are split into the three subgroups US (*top*), UCL (*middle*), and LCC (*bottom*). The primary stars are indicated with circles; the confirmed companions with large squares, and the candidate companions with small squares. The M_{K_S} magnitude is derived from the K_S magnitude by correcting for distance and extinction for each target individually. The solid curves represent isochrones of 5 Myr (for US) and 20 Myr (for UCL and LCC). The 15 Myr and 23 Myr isochrones enclose the gray-shaded area and represent the uncertainty in the age of the UCL and LCC subgroups. For each data point we indicate the 1σ errors. The photometry of the observed objects cannot be used to distinguish between the subgroups of Sco OB2, due to the errors and the small sample. The free-floating brown dwarfs in US identified by Martín et al. (2004) are indicated with triangles, adopting a distance of 145 pc.

Chabrier et al. (2000) for $0.02\ M_\odot \leq M < 1\ M_\odot$, Palla & Stahler (1999) for $1\ M_\odot \leq M < 2\ M_\odot$, and Girardi et al. (2002) for $M > 2\ M_\odot$. For members of the US subgroup we use the 5 Myr isochrone, and for UCL and LCC members we use the 20 Myr isochrone.

Absolute magnitudes M_J, M_H, and M_{K_S} are derived from the apparent magnitudes using for each star individually the parallax and interstellar extinction A_V from de Bruijne (1999); see Kouwenhoven et al. (2005) for details. The error on the parallax is 5−10% for all targets, and can therefore be used to derive reliable distances to individual stars (e.g., Brown et al. 1997). The median fractional error on the distance is 6.5%, which introduces an additional error of 0.15 mag on the absolute magnitudes. Combining this error with the error in the apparent magnitude (Sect. 2.6) we obtain 1σ error estimates for the absolute magnitudes of 0.16 mag for the primaries, 0.17 mag for the bright companions, and 0.19 mag for the faint companions. The colors are directly calculated from the apparent magnitudes, and are not affected by parallax errors.

The color–magnitude diagrams (with *absolute* magnitudes) for the subgroups are shown in Fig. 5. The measurements for US are in the top panels, and those of UCL and LCC are in the middle and bottom panels, respectively. The curves represent the 5 Myr (for US) and 20 Myr (for UCL and LCC) isochrones. The gray-shaded area indicates the inaccuracy in isochrone placement due to the age uncertainty in the subgroups (∼1 Myr for US members, ∼4 Myr for UCL/LCC members; see Table 1). Due to our small sample and the errors in the photometry we cannot see a difference between the magnitude and color distributions of the three subgroups. For comparison we have included the free-floating brown dwarf candidates in US reported by Martín et al. (2004).

4.2. Distinction between companions and background stars

Individual distances to Sco OB2 member stars are available (de Bruijne 1999), as well as the ages of the three subgroups of Sco OB2. A companion of a Sco OB2 member star has (by definition) practically the same distance as its primary. It is very likely that a primary and companion in Sco OB2 are coeval. The probability that a companion is captured dynamically is very small, since this involves either a multiple-star interaction or significant tidal dissipation. It is even less likely that the companion is a captured field star, i.e., that the primary and companion have a different age. Background stars generally have a different age, distance, or luminosity class than Sco OB2 members. In principle it is possible that an ADONIS or NACO field contains two members of the Sco OB2 association at different distances due to projection effects, but Kouwenhoven et al. (2005) showed that this effect can be neglected. Physical companion stars thus have the same age and distance as their primary, and therefore should fall on the isochrone for the subgroup to which the primary belongs, contrary to background stars. We use this property to separate physical companions and background stars.

For each stellar component we determine in the color–magnitude diagram (Fig. 5) the point on the isochrone that corresponds best to the measured position. The differences in color and magnitude of the star and the nearest point on the isochrone are then compared to the observational errors. We use the χ^2 test to determine how compatible the observed color and magnitude of a secondary are with the isochrone. For example, if the best-fitting value in the $(J-K_S, M_{K_S})$-diagram deviates by $\Delta(J-K_S)$ in color and by ΔM_{K_S} in magnitude from the isochrone, the χ^2 value is given by

$$\chi^2 = \frac{[\,\Delta(J-K_S)\,]^2}{\sigma^2_{J-K_S} + \sigma^2_{J-K_S,\mathrm{iso}}} + \frac{\Delta M^2_{K_S}}{\sigma^2_{M_{K_S}} + \sigma^2_{M_{K_S},\mathrm{iso}}} \quad (1)$$

where σ_{J-K_S} and $\sigma_{M_{K_S}}$ are the observational errors in color and absolute magnitude, respectively. The errors on the location of the isochrone (due to age and metallicity uncertainty) are denoted with $\sigma_{J-K_S,\mathrm{iso}}$ and $\sigma_{M_{K_S},\mathrm{iso}}$. The age uncertainty is ∼1 Myr for members of US and ∼4 Myr for members of UCL and LCC (see Table 1). The error in the placement of the corresponding isochrones due to age uncertainty is shown in Fig. 5, and is small compared to the photometric errors. We assume a solar metallicity for all observed stellar components. The metallicity [M/H] of Sco OB2 has not been studied in detail. In their metallicity study of Ori OB2, Cunha & Lambert (1994) found a metallicity slightly (∼0.2 dex) lower than solar for this association. Using the models of Siess et al. (2000) we estimate that the metallicity uncertainty Δ[M/H] = 0.2 results in an additional isochronal error of 0.05 mag in JHK_S and 0.06 mag in the colors of low-mass ($M \lesssim 0.5\ M_\odot$) companions.

The χ^2 values for the secondaries in each of the three color–magnitude diagrams are listed in Table A.2 (as long as they are available). For the classification into companions and background stars we consider the *largest* of the three χ^2 values available for each secondary. We choose this strategy (instead of, e.g., taking the average χ^2 value), because background stars may be consistent with the isochrone for e.g. $J-K_S$, but not for $H-K_S$. The physical companions, however, should be consistent with the isochrone in all color–magnitude diagrams (within the error bars).

Table 3 lists the criteria we adopt to classify the secondaries into three groups: confirmed companions, candidate companions, and background stars. The χ^2 value of 2.30 corresponds to the 1σ confidence level, which means that statistically 68.3% of the companion stars have $\chi^2 < 2.30$. Similarly, 99.73% of the companions have $\chi^2 < 11.8$ (3σ confidence level). The above confidence levels are for a dataset with two degrees of freedom, under the assumption that the errors are Gaussian (Press et al. 1992).

Table 3. Criteria adopted to separate the secondaries with multi-color observations into confirmed companions, candidate companions, and background stars. The χ^2 values of 2.30 and 11.8 correspond to the 1σ and 3σ levels. This means that (statistically) 68.3% of the physical companions have $\chi^2 < 2.30$ and 99.73% of the physical companions have $\chi^2 < 11.8$. A secondary with $\chi^2 < 2.30$ is very likely a companion star. A secondary with $\chi^2 > 11.8$ is almost certainly a background star. The secondaries with $2.30 < \chi^2 < 11.8$ may be companions or background stars.

Secondary status	Symbol	Criterion
Confirmed companion	c	$\chi^2 \leq 2.30$
Candidate companion	?	$2.30 < \chi^2 \leq 11.8$
Background star	b	$11.8 < \chi^2$

For several objects we have lower limits on the magnitudes in one or two of the filters. Using the lower limits on J, H, or K_S we calculate upper or lower limits on χ^2 and are able to classify several additional objects as background stars.

Even though we are sensitive (although not complete) to massive planets around our NACO targets, we do not classify the very faint secondaries in this paper, for two reasons. First, many faint background stars are expected in the ADONIS and NACO field of view (see Sect. 4.3). Due to the larger error bars for faint secondaries, several background stars may be consistent with the isochrone; the vast majority of the "candidate planets" are likely background stars. Second, the presently available evolutionary models for massive planets are not very reliable for young ages (see e.g., Chabrier et al. 2005, for a review). Throughout our analysis we do not consider objects with a mass below 0.02 $M_\odot$. Consequently, all secondaries with an inferred mass smaller than 0.02 $M_\odot$ are classified as background stars.

The status given to each secondary is listed in Table A.2. The secondaries with $\chi^2 < 2.30$ are very likely companions because of their proximity to the isochrone. As statistically only 1 out of 370 companions have $\chi^2 > 11.8$, we claim with high confidence that the secondaries with $\chi^2 > 11.8$ are background stars. We cannot confirm the status of the secondaries with $2.30 < \chi^2 < 11.8$. These secondaries are consistent with the isochrone within the 3σ error bars. However, due to the large number of faint background stars, it is likely that several background stars also satisfy this criterion. As we cannot confirm either their companion status or their background star status, we will refer to the secondaries with $2.30 < \chi^2 < 11.8$ as candidate companions.

The properties of the 25 confirmed companion stars found around the 22 members in the NACO survey and the 9 members with multi-color observations in the ADONIS survey are listed in Table 4. Table 5 lists the distribution of confirmed and candidate companions over angular separation ρ and K_S magnitude. The largest fraction of candidate companions (relative to the number of confirmed companions) is seen for faint secondaries at large angular separation. In Sect. 6 we will study the virtual absence of companions with $1'' \leq \rho \leq 4''$ and $12 \leq K_S \leq 14$ mag. Table 5 shows that only one confirmed companion is detected in this region; no candidate companions are found.

Table 4. Properties of the 25 confirmed companion stars found around the 22 members in our NACO survey and the 9 members with multi-color observations in the ADONIS survey. The columns show the secondary designation, the J, H, and K_S magnitudes, the angular separation, and the position angle (measured from North to East). Magnitude lower limits are given if a secondary is not detected in a filter. We list the absolute magnitude and corresponding mass in columns 7 − 10. The 11th column lists the status of the object (c = confirmed companion star, nc = new confirmed companion star). The last column shows additional remarks. A "J", "H", or "K" means that the secondary flux in this filter was obtained from the image obtained *without* the NDF, using the PSF from the corresponding image that was obtained *with* NDF (see Sect. 2.4). Properties of the observed primaries, candidate companions, and background stars are not shown here; these are listed in Table A.1.

Star	J	H	K_S	ρ	PA	M_J	M_H	M_{K_S}	Mass	Status	Remarks
	mag	mag	mag	arcsec	deg	mag	mag	mag	$M_\odot$		
NACO targets											
HIP 59502 -1	12.35	11.83	11.64	2.94	26.39	7.39	6.86	6.68	0.14	c	
HIP 62026 -1	8.08	7.90	7.86	0.23	6.34	2.88	2.71	2.66	1.19	c	
HIP 63204 -2	8.79	8.51	8.40	0.15	236.56	3.59	3.31	3.19	1.06	c	
HIP 67260 -1	8.88	8.46	8.36	0.42	229.46	3.42	2.99	2.90	1.10	c	
HIP 67919 -1	9.98	9.38	9.10	0.69	296.56	4.89	4.30	4.02	0.75	c	
HIP 68532 -1	10.52	9.85	9.54	3.05	288.50	5.03	4.36	4.05	0.73	c	
HIP 68532 -2	11.38	10.94	10.63	3.18	291.92	5.89	5.45	5.14	0.39	c	
HIP 69113 -1	10.98	10.43	10.29	5.34	65.15	4.83	4.28	4.14	0.77	c	
HIP 69113 -2	11.27	10.45	10.30	5.52	67.17	5.12	4.29	4.15	0.72	c	
HIP 73937 -1	>8.40	8.46	8.37	0.24	190.58	>2.94	3.00	2.91	1.11	c	
HIP 79739 -1	12.28	11.52	11.23	0.96	118.33	6.34	5.58	5.29	0.16	c	
HIP 79771 -1	12.00	11.28	10.89	3.67	313.38	6.06	5.33	4.94	0.19	c	
HIP 79771 -2	12.39	11.79	11.42	0.44	128.59	6.44	5.85	5.47	0.13	nc	
HIP 80799 -1	10.60	10.04	9.80	2.94	205.02	5.08	4.51	4.27	0.34	c	
HIP 80896 -1	11.16	10.63	10.33	2.28	177.23	5.60	5.07	4.77	0.24	c	
HIP 81972 -3	12.54	11.86	11.77	5.04	213.45	6.16	5.48	5.39	0.35	c	J
HIP 81972 -4	15.10	14.43	13.98	2.79	106.94	8.72	8.05	7.60	0.06	nc	JHK
HIP 81972 -5	16.11	15.63	15.26	7.92	229.27	9.73	9.25	8.88	≈0.03	nc	JHK
ADONIS multi-color subset											
HIP 76071 -1	>11.25	11.28	10.87	0.69	40.85	>5.09	5.12	4.71	0.23	c	
HIP 77911 -1	12.68	12.20	11.84	7.96	279.25	6.82	6.34	5.98	0.09	c	
HIP 78809 -1	11.08	10.45	10.26	1.18	25.67	5.32	4.69	4.50	0.30	c	
HIP 78956 -1	9.76	9.12	9.04	1.02	48.67	3.39	2.75	2.67	1.16	c	
HIP 79124 -1	11.38	10.55	10.38	1.02	96.18	5.33	4.50	4.33	0.33	c	
HIP 79156 -1	11.62	10.89	10.77	0.89	58.88	5.50	4.77	4.65	0.27	c	
HIP 80238 -1	7.96	7.66	7.49	1.03	318.46	2.34	2.04	1.87	1.67	c	

Table 5. The distribution of companion stars over angular separation ρ and K_S magnitude for our sample of 31 targets with multi-color observations. Each entry lists the number of confirmed companion stars, i.e., the secondaries with $\chi^2 < 2.30$. Between brackets we list the number of candidate companion stars, which have $2.30 < \chi^2 < 11.8$. We have also included the candidate companion HIP 80142-2 ($\rho = 5.88''$), for which no K_S measurement is available. Several candidate companions are likely to be background stars, especially faint candidates at large separation. In the region $1'' \leq \rho \leq 4''$ and 12 mag $\leq K_S \leq$ 14 mag (which we will study in Sect. 6) we find one confirmed companion and no candidate companions.

	$\rho < 1''$	$1'' \leq \rho \leq 4''$	$\rho > 4''$	Total
$K_S < 12$ mag	9 (−)	10 (2)	4 (2)	23 (4)
$12 \leq K_S \leq 14$ mag	− (−)	1 (−)	− (1)	1 (1)
$K_S > 14$ mag	− (−)	− (3)	1 (3)	1 (6)
no K_S available	− (−)	− (−)	− (1)	− (1)
Total	9 (−)	11 (5)	5 (7)	25 (12)

4.3. The background star population

Our method to separate companions and background stars is based on a comparison between the location of the secondaries in the color–magnitude diagrams and the isochrone. The number of background stars identified with this method should be comparable to the *expected* number of background stars in the fields around the targets. In this section we make a comparison between these numbers, where the expected number of background stars is based on (1) the Besançon model of the Galaxy, and (2) the background star study in Sco OB2 performed by Shatsky & Tokovinin (2002).

We use the Besançon model of the Galaxy (Robin et al. 2003) to characterize the statistical properties of the background star population. We obtain star counts in the direction of the centers of the three subgroups, as well as for $(l, b) = (300°, 0°)$, where LCC intersects the Galactic plane. We include objects of any spectral type, luminosity class, and population, up to a distance of 50 kpc, and convert the model K magnitude to K_S magnitude. As expected, the Besançon model shows a strong variation in the number of background stars with Galactic latitude. Most background stars are found in the direction of the Galactic plane. For a given numerical value of the magnitude limit, more background stars are expected to be found in the K_S band than in the J and H bands. Although the Besançon model is in good agreement with the observed properties of the Galaxy, it cannot be used to make accurate predictions for individual lines of sight. For example, the high variability of the interstellar extinction with the line-of-sight, which is known to be important for the background star statistics (Shatsky & Tokovinin 2002), is not taken into account in the Besançon model. A high interstellar extinction reduces the observed number of background stars significantly, which is especially important for the US subgroup, which is located near the ρ Oph star forming region.

Let $F(K_S)$ be the number of background stars brighter than K_S, per unit of surface area. Above we mentioned that the number of background stars in the Besançon model, i.e., the normalization of $F(K_S)$, varies strongly with Galactic coordinates.

The profile of $F(K_S)$, however, is very similar for different lines of sight, and can be approximated with a function of the form $F(K_S) = C_i \times 10^{\gamma \cdot K_S}$, with $\gamma = 0.32 \pm 0.01$ for $5 \leq K_S \leq 20$ mag. The constant C_i defines the normalization of $F(K_S)$, which depends on the Galactic coordinates.

The number of background stars within a certain angular separation ρ is proportional to the enclosed area $A(\rho)$ in the field of view within that angular separation. For our NACO observations we have a square detector of size $L_{\rm NACO} = 14$ arcsec; for the observing strategy we used for the ADONIS observations we effectively have $L_{\rm ADO} = \frac{3}{2} \cdot 12.76$ arcsec (see Kouwenhoven et al. 2005). For a given ρ (in arcsec) the enclosed area (in arcsec^2) is then given by

$$A_i(\rho) = \begin{cases} \rho^2 & \text{for } \rho \leq L_i/2 \\ \pi\rho^2 - 4\rho^2 \arccos\left(L_i/2\rho\right) + L_i \sqrt{4\rho^2 - L_i^2} & \\ & \text{for } L_i/2 < \rho \leq L_i/\sqrt{2} \\ L_i^2 & \text{for } \rho > L_i/\sqrt{2}, \end{cases} \quad (2)$$

where the subscript i refers to either the ADONIS or the NACO observations. Here we make the assumption that the target star is always in the center of the field of view. In our NACO survey we occasionally observe the target star off-axis in order to study a secondary at angular separation larger than $L_{\rm NACO}/\sqrt{2} = 9.9''$, but we ignore this effect here.

We now have expressions for the quantity $N(K_S, \rho)$, the expected number of background stars with magnitude brighter than K_S and angular separation smaller than ρ, as a function of K_S and ρ:

$$N_i(K_S, \rho) = F(K_S) \cdot A_i(\rho) = C_i \cdot 10^{\gamma \cdot K_S} \cdot A_i(\rho), \quad (3)$$

where $\gamma = 0.32 \pm 0.01$, $A(\rho)$ is defined in Eq. (2), and C_i is a normalization constant.

For the normalization of Eq. (3) we compare our observations with the background star study of Shatsky & Tokovinin (2002). Apart from their target observations, the authors additionally obtained sky images centered at 21 arcsec from each target in order to characterize the background star population. >From the background star study of Shatsky & Tokovinin (2002) we derive the expected number of background stars in the ADONIS and NACO field of view. We assume a detection limit of $K_S = 15$ mag for ADONIS and $K_S = 17$ mag for NACO (which roughly corresponds to the completeness limit of the background star study of Shatsky & Tokovinin 2002). Using the data from the background star study of Shatsky & Tokovinin (2002) we calculate the expected number of background stars for each ADONIS and NACO field, for the three subgroups and for targets close to the Galactic plane ($|b| < 5°$). Table 6 lists the expected number of background stars with corresponding Poisson errors. Additionally, we list the number of targets observed in each of the four regions. For the 177 targets observed with ADONIS *only* we expect ≈71 background stars, and for the 22 targets observed with NACO we expect ≈19 background stars. In our combined ADONIS and NACO dataset, the expected number of background stars is 90 ± 6. This gives normalization factors $C_{\rm ADONIS} = 1.74 \times 10^{-8}$ arcsec^{-2} and $C_{\rm NACO} = 1.60 \times 10^{-8}$ arcsec^{-2} for Eq. (3).

Figure 6 shows the expected number of background stars brighter than K_S and closer than ρ as a function of K_S and ρ, for the combined ADONIS and NACO dataset. Since most of our targets are observed with ADONIS only, the shape of the expected background star density distribution is dominated by that of ADONIS. As we have a square field of size

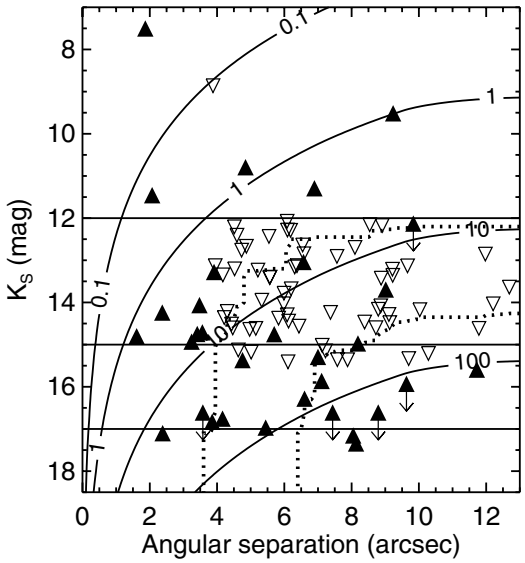

Fig. 6. The *expected* number of background stars brighter than K_S at angular separation smaller than ρ for the combined sample of 199 targets (solid contours). Overplotted are the background stars detected around the 22 NACO targets (filled triangles), and those found around the 177 targets observed with ADONIS *only* (open triangles). The *observed* cumulative number of background stars is indicated with the dotted contours, for values of 10 and 50 background stars, respectively. In Kouwenhoven et al. (2005) we classify secondaries brighter than $K_S = 12$ mag (upper horizontal line) as candidate companions, and those fainter than $K_S = 12$ mag as probable background stars. The faintest objects we detect in our ADONIS and NACO surveys have K_S magnitude of approximately 15 and 17 magnitudes, respectively (lower horizontal lines).

Table 6. The number of background stars *expected* in our ADONIS and NACO fields of view, based on the background star study of Shatsky & Tokovinin (2002). Column 1 lists the four regions for which we study the background statistics. The targets with Galactic latitude $|b| \leq 5°$ are included in the region GP. The other targets are grouped according to their membership of US, UCL, and LCC. For the 177 targets *only* observed with ADONIS and the 22 targets observed with NACO we list the expected number of background stars per field of view, and the number of targets observed in the four regions. In total we expect to find 70.75 ± 4.90 background stars in the ADONIS sample, and 18.96 ± 3.96 in the NACO sample.

	ADONIS		NACO	
Region	stars per field	$N_{\rm fields}$	stars per field	$N_{\rm fields}$
US	$0.06^{+0.06}_{-0.02}$	51	$0.10^{+0.11}_{-0.04}$	9
UCL	$0.27^{+0.06}_{-0.02}$	64	$0.47^{+0.11}_{-0.10}$	3
LCC	0.43 ± 0.08	40	0.73 ± 0.14	5
GP	1.51 ± 1.03	22	2.59 ± 1.76	5
Total		177		22

$L_{\rm ADO} = 19.1$ arcsec, the cumulative number of background stars rises rapidly between $\rho = 0''$ and $\rho = L_{\rm ADO}/\sqrt{2} = 13.5''$ and becomes flat for larger separations. The background stars from the NACO survey are represented with the filled triangles, and those detected *only* in the ADONIS survey are represented with open triangles. Figure 6 shows that the (ρ, K_S) distribution of the observed 97 background stars is in good agreement with that of the expected 90 background stars. In the extreme case that all 12 candidate companions are actually background stars, the observed number of background stars is 110. In this extreme case there are 22% more background stars than expected, which

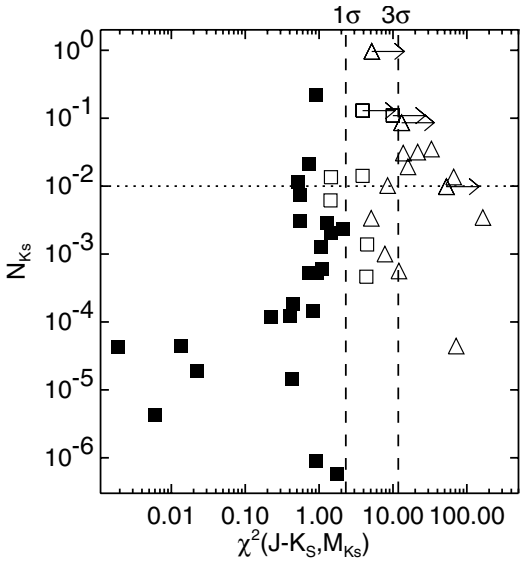

Fig. 7. The χ^2 distance to the isochrone in the $(J - K_S, M_{K_S})$ diagram versus $N(K_S, \rho)$, where $N(K_S, \rho)$ is the expected number of background stars brighter than K_S and angular separation smaller than ρ. The vertical dashed lines correspond to $\chi^2 = 2.30$ (1σ; *left*) and $\chi^2 = 11.8$ (3σ; *right*). The symbols represent the confirmed companions (filled squares), the candidate companions (open squares), and background stars (triangles). Note that the classification of a secondary is based on the χ^2 values for the different color–magnitude diagrams; not only for the χ^2 of the $(J - K_S, M_{K_S})$-diagram, which is shown above. The expected number of background stars in a field (vertical axis) is used as a consistency check. The horizontal dotted line represents the 1% filter used by Poveda et al. (1982) to separate companion stars (below the line) and background stars (above the line). The 1% filter is a reasonable method when multi-color observations are not available, but is not used in our study. The triangle in the lower-right quadrant represents HIP 63204-1 (see Sect. 4.4).

suggests that a significant part of the candidate companions may indeed be physical companions.

Background stars are by definition not associated with the target star, and therefore generally have (1) a random position in the field of view of the observation, and (2) a position in the color–magnitude diagram that is likely to be inconsistent with the isochrone. Figure 7 shows the relation between $N(K_S, \rho)$ and the χ^2 value derived from the location of the secondary in the $(J - K_S, M_{K_S})$ diagram with the isochrone. In other words, Fig. 7 shows the probability of detecting a background star at separation ρ (or smaller) and magnitude K_S (or brighter) versus how far away the secondary is from the isochrone. The vertical dashed lines in Fig. 7 are at $\chi^2 = 2.30$ and $\chi^2 = 11.8$, the values used to determine the status of the companions (see Table 3). This correlation provides additional support to the method we use to separate companions and background stars.

Poveda et al. (1982) performed a statistical study of binary stars in the Index Catalogue of Visual Double Stars. They showed that it is statistically plausible to assume that components with $N(\rho, m_2) > 0.01$ are background stars, where m_2 is the magnitude of the secondary. This technique is referred to as the "1% filter". The horizontal line in Fig. 7 represents the 1% filter used by Poveda et al. (1982). Secondaries below this line would be classified as companions using the 1% filter, and those above would be classified as background stars. Figure 7 shows that the 1% filter is a reasonable technique, but not as accurate as the multi-color technique used in this paper.

4.4. Notes on some individual secondaries

We detect two hierarchical triple systems: HIP 68532 and HIP 69113. The two companions of HIP 68532 (previously reported in Kouwenhoven et al. 2005) have a mass of 0.73 $M_\odot$ and 0.39 $M_\odot$, respectively. HIP 68532 has a companions-to-primary mass ratio of (0.73+0.39)/1.95 = 0.57. The companions are separated 0.23″ (~28 AU) from each other and 3.11″ (~385 AU) from the primary, giving an estimate of 0.073 for the ratio between the semi-major axes of the inner and outer orbits. The two companions of HIP 69113 (previously reported in Huélamo et al. 2001) have a mass of 0.77 $M_\odot$ and 0.72 $M_\odot$, respectively, corresponding to a companions-to-primary mass ratio of 0.39. The companions are separated 0.26″ (~44 AU) from each other and 5.43″ (~917 AU) from the primary, giving an estimate of 0.048 for the ratio between the semi-major axes of the inner and outer orbits.

For HIP 62026-1 we find a significant difference in position angle between the ADONIS and NACO observations. With the ADONIS observations, obtained on 8 June 2001, we find $(\rho, \varphi) = (0.22'', 12.5°)$. With NACO we measure $(\rho, \varphi) = (0.23'', 6.34°)$, 1033 days later. As the angular separation between HIP 62026-1 and its primary is small, the observed position angle difference may well be the result of orbital motion. Assuming a circular, face-on orbit, we estimate an orbital period of 165 year for the system HIP 62026. The total mass of the system (taken from Table A.1) is 3.64 ± 0.25 $M_\odot$, which gives via Kepler's law a semi-major axis of 46 AU. This value is of the same order of magnitude as the (projected) semi-major axis of ~24 AU derived from the angular separation of 0.22″ between the components (adopting a distance of 109 pc to HIP 62026).

HIP 63204-1 is a bright and red object separated only 1.87 arcsec from the LCC member HIP 63204. The isolated location of HIP 63204-1 in the bottom-right quadrant of Fig. 7 shows that the probability of finding a background star of this magnitude (or brighter) at this angular separation (or closer) is small. According to its location in the color–magnitude diagrams, HIP 63204-1 is a background star and hence we classify it as such. HIP 63204 and its companion HIP 63204-2 at $\rho = 0.15''$ have masses of 2.05 $M_\odot$ and 1.06 $M_\odot$, respectively. If HIP 63204-1 (at $\rho = 1.87''$) would be a companion, its mass would be approximately 1 $M_\odot$, in which case HIP 63204 would be an unstable triple system. The colors of HIP 63204-1 are consistent with a 0.075 $M_\odot$ brown dwarf with an age of 10 Gyr at a distance of 60 pc, and are also consistent with those of an M5 III giant at a distance of ~5.6 kpc (using the models of Cox 2000; Chabrier et al. 2000).

HIP 81972-3, HIP 81972-4, and HIP 81972-5 fall on the 20 Myr isochrone in all three color–magnitude diagrams. These objects are likely low-mass companions of HIP 81972 (see Sect. 5). HIP 81972-5 is the topmost companion (black square) in Fig. 7. HIP 81972-5 is the faintest companion in our sample, and the expected number of background stars with a similar or brighter magnitude and a similar or smaller separation is large (~16 for the ADONIS sample). The secondary HIP 81972-2 (at $\rho = 7.02''$) was reported before as a possible companion of HIP 81972 in Worley & Douglass (1997), but the secondary is classified as a background star by Shatsky & Tokovinin (2002). With our NACO multi-color observations we cannot determine the nature of this secondary with high confidence. The LCC member HIP 81972 is located close to the Galactic equator ($b = +3°11'$), so care should be taken; background stars with a magnitude similar to that of the secondaries of HIP 81972 are expected in the field around this star.

Table 7. Accuracy of the $K_S = 12$ mag criterion to separate companions and background stars. This table contains 69 out of the 72 secondaries with multi-color observations in the ADONIS or NACO dataset. Three secondaries (1 candidate companion; 2 background stars) for which no K_S magnitudes are available, are not included. The first column shows the status of the secondary (c = confirmed companion, ? = candidate companion, b = background star). Columns 2 to 5 list the distribution over status for secondaries with $K_S < 12$ mag and $K_S > 12$ mag. Depending on the true nature of the candidate companion stars, the $K_S = 12$ mag criterion correctly classifies the secondaries in ~80% of the cases.

Status	$K_S < 12$ mag		$K_S > 12$ mag		Total
c	23	(70%)	2	(6%)	25
?	4	(12%)	7	(19%)	11
b	6	(18%)	27	(75%)	33
Total	33	(100%)	36	(100%)	69

Kouwenhoven et al. (2005) identified seven "close background stars" ($K_S > 14$ mag; $\rho < 4''$), for which the background star status was derived using the K_S magnitude only. These are objects next to the targets HIP 61265, HIP 67260, HIP 73937, HIP 78958, HIP 79098, HIP 79410, and HIP 81949. The ADONIS observations are incomplete in this region (see Fig. 3). More low-mass companions with $K_S > 14$ mag and $1'' < \rho < 4''$ may be present for the 177 A and late-B stars *only* observed with ADONIS.

With our NACO multi-color observations we confirm that five of the "close background stars" (HIP 61265-2, HIP 73937-2, HIP 79098-1, 79410-1, and HIP 81949-2) are background stars. For the other two secondaries, HIP 67260-3 and HIP 78969-1, we cannot determine whether they are background stars or brown dwarf companions. As many background stars with similar magnitudes are expected in the field, these are likely background stars. However, follow-up spectroscopic observations are necessary to determine the true nature of these close secondaries.

4.5. Accuracy of the $K_S = 12$ separation criterion

One of the goals of our study is to evaluate the accuracy of the $K_S = 12$ mag criterion that we used to separate companions and background stars in the ADONIS survey. This is possible, now that we have performed a multi-color analysis of 72 secondaries around 31 members of Sco OB2. Table 7 shows the distribution of secondary status for the secondaries with $K_S < 12$ mag and those with $K_S > 12$ mag (three secondaries without K_S measurements are not included). According to the $K_S = 12$ criterion, all secondaries brighter than $K_S = 12$ mag are companions, while all fainter secondaries are background stars.

If we consider only the confirmed companions and background stars, we see that the $K_S = 12$ mag criterion correctly classifies the secondaries in $f = (23 + 27)/(25 + 33) = 86\%$ of the cases. If all candidate companions are indeed companions, we have $f = 78\%$, while if all candidate companions are background stars, we have $f = 82\%$. This indicates that ~80% of the candidate companions identified by Kouwenhoven et al. (2005) are indeed companion stars.

The $K_S = 12$ mag criterion is accurate for the measured set of secondaries *as a whole*. It is obvious that for the lowest-mass companions the criterion is not applicable, as virtually all brown dwarf and planetary companions have $K_S > 12$ mag at the distance of Sco OB2. Out of the 25 confirmed companions we find with our multi-color analysis, 23 indeed have $K_S < 12$ mag, but two have $K_S > 12$ mag. These are the brown dwarf companions of HIP 81972 (see Sects. 4.2 and 5 for a discussion).

Now that we have confirmed the validity of the $K_S = 12$ mag criterion, many of the candidate companions found in the ADONIS survey very likely are physical companion stars. Table A.3 gives an overview of all candidate and confirmed companion stars identified in the ADONIS and NACO surveys.

5. Masses and mass ratios

For each primary and companion star we derive the mass using its color and magnitude. We find the best-fitting mass by minimizing the χ^2 difference between the isochrone and the measurements, while taking into account the errors in the measurements:

$$\chi^2 = \left(\frac{\Delta(J-K_S)}{\sigma_{J-K_S}}\right)^2 + \left(\frac{\Delta(H-K_S)}{\sigma_{H-K_S}}\right)^2 + \left(\frac{\Delta M_{K_S}}{\sigma_{M_{K_S}}}\right)^2. \quad (4)$$

The masses of all primaries and confirmed companions are listed in Table A.1. We additionally list the masses of the candidate companions, assuming that they are indeed companions, but we do not include these masses in our analysis. We find primary masses between 1.1 $M_\odot$ and 4.9 $M_\odot$. The confirmed companion star masses range between 0.03 $M_\odot$ and 1.19 $M_\odot$, with mass ratios $0.006 < q < 0.55$. The average error in the mass as a result of the error in the color and magnitude is 8.5% for the primaries and 12% for the companion stars. The average error in the mass ratio is 12.5%. Although accurate B and $B - V$ measurements are available for the primaries, we do not use these. The B and V measurements often include the flux of unresolved close companions, and therefore lead to overestimating the primary masses.

Kouwenhoven et al. (2005) derived masses from K_S magnitudes only. For the primary stars these are close to those obtained from multi-color observations in our current analysis. The rms difference between the masses derived using the two methods is 6.6%. No systematic difference is present for the primaries. Kouwenhoven et al. (2005) overestimated the companion star masses with ~2.2% (~0.01 $M_\odot$) on average.

The companions with the lowest mass are those of HIP 81972, which have masses of 0.35 $M_\odot$ (370 M_J), 0.06 $M_\odot$ (63 M_J), and 0.03 $M_\odot$ (32 M_J). The latter two are likely brown dwarfs. With an angular separation of $\rho = 2.79''$, the 63 M_J component is the only observed brown dwarf in the $1'' - 4''$ angular separation interval (see Sect. 6). The other two companions of HIP 81972 have a larger angular separation.

6. The lower end of the companion mass distribution

Kouwenhoven et al. (2005) discussed the potential lack of substellar companions to A and late-B members of Sco OB2. With our NACO follow-up observations we confirm the very low number of brown dwarf companions with respect to the number of stellar companions found around these stars (Sect. 6.1). In Sect. 6.2 we will discuss whether a brown dwarf desert exists among A and late-B members of Sco OB2. In Sect. 6.3 we will briefly discuss the potential origin of such a brown dwarf desert. We will show that the small brown dwarf companion fraction among A- and B stars in Sco OB2 can be explained by an extrapolation of the *stellar* companion mass distribution, i.e., there is no need to eject brown dwarf companions from binary systems at an early stage of the formation process (the embryo ejection scenario; Reipurth & Clarke 2001).

6.1. The brown dwarf "gap" for $1'' \leq \rho \leq 4''$

Kouwenhoven et al. (2005) observed a gap in the (ρ, K_S) distribution of the stellar companions in the Sco OB2 binary population: no secondaries with a magnitude 12 mag $\leq K_S \leq$ 14 mag and an angular separations $\rho < 4''$ were detected. These secondaries should have been detected, had they existed, since the ADONIS survey is almost complete in this region (see Fig. 3). Figure 8 shows the distribution of K_S and ΔK_S as a function of ρ for the ADONIS and NACO observations combined. The "gap" in the (ρ, K_S) distribution described above is clearly visible. With our NACO survey we detect one companion at the bottom of this region: the brown dwarf companion HIP 81972-4 ($K_S = 13.98 \pm 0.12$ mag; see also Sects. 4.2 and 5). No other secondaries are present in this region.

The stellar companion fraction is the fraction of stars with stellar companions. Among A and late-B stars in Sco OB2 in the semi-major axis range $1'' - 4''$ (130 – 520 AU) we find a stellar companion fraction of $14 \pm 3\%$. Similarly, the brown dwarf companion fraction is the fraction of stars with brown dwarf companions. The brown dwarf companion fraction for the stars in this separation range is $0.5 \pm 0.5\%$[4] (for brown dwarfs with $K_S < 14$ mag). The substellar-to-stellar companion ratio R is defined as

$$R = \frac{\text{number of brown dwarf companions}}{\text{number of stellar companions}}. \quad (5)$$

In our study we cannot calculate R because we do not know how many faint ($K_S > 14$ mag) brown dwarf companions are missing. We therefore calculate the *restricted* substellar-to-stellar companion ratio $R_\star$, using only the brown dwarf companions brighter than $K_S = 14$ mag[5]. In the angular separation range $1'' - 4''$ we observe $R_{\star,\mathrm{IM}} = 0.036 \pm 0.036$ for intermediate mass stars in Sco OB2. We cannot make similar statements for companions with properties other than those described above. For angular separations smaller than $1''$ our survey is significantly incomplete for 12 mag $\leq K_S \leq$ 14 mag. For $\rho > 4''$ many objects with 12 mag $\leq K_S \leq$ 14 mag are likely background stars, of which the status still needs to be confirmed. Finally, the ADONIS survey is incomplete for $K_S > 14$ mag.

6.2. A real brown dwarf desert?

The brown dwarf desert is defined as a deficit (not necessarily a total absence) of brown dwarf companions, either relative to the frequency of companion stars or relative to the frequency of planetary companions (McCarthy & Zuckerman 2004). In this paper the brown dwarf desert for A and late-B members of Sco OB2 is characterized by a small number of observed companions $N_{\star,\mathrm{BD}}$ with 12 mag $\leq K_S \leq$ 14 mag and $1'' \leq \rho \leq 4''$ and a small substellar-to-stellar companion ratio $R_\star$ (where the star in the subscript refers to the *observed* quantities). In general, the quantities N_{BD} and R depend on (1) the mass distribution, (2) the pairing properties of the binary systems, and (3) the spectral type of the stars in the sample. Unlike R, the value of N_{BD} also depends on (4) the multiplicity fraction F_{M} (Eq. (9)), and (5) the semi-major axis (or period) distribution. We use simulated observations and compare the observed values with those predicted for various models, in order to roughly estimate the mass distribution and pairing properties. For comparison between observations and simulations we only consider the companions brighter than $K_S = 14$ mag in the angular separation range $1'' \leq \rho \leq 4''$.

We simulate models using the STARLAB package (e.g., Portegies Zwart et al. 2001). The primary mass is drawn in the mass range $0.02\ M_\odot \leq M \leq 20\ M_\odot$, either the Salpeter mass distribution

$$f_{\mathrm{M}}(M) = \frac{\mathrm{d}M}{\mathrm{d}N} \propto M^{-2.35}, \quad (6)$$

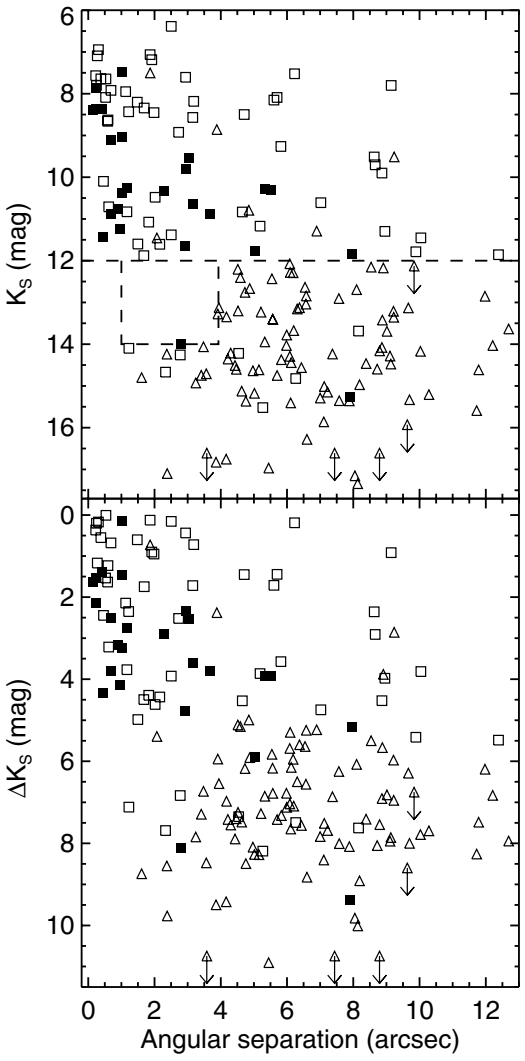

Fig. 8. Companion star magnitude K_S (*top*) and magnitude difference ΔK_S (*bottom*) versus angular separation for the combined ADONIS and NACO datasets. The symbols represent confirmed companions (filled squares), candidate companions (open squares), and background stars (triangles); see Sect. 4.2 for further information on this classification. The horizontal line corresponds to $K_S = 12$ mag, the criterion used by Kouwenhoven et al. (2005) to separate companion stars and background stars. Typical detection and completeness limits corresponding to the observations are shown in Fig. 3. For a given K_S magnitude, the number of background stars closer than angular separation ρ is given by Eq. (3). This figure clearly shows the dearth of brown dwarf companions with $1'' < \rho < 4''$ around A and late-B stars in Sco OB2 (region indicated with the dashed rectangle).

[4] Note that we only find one brown dwarf companion with 12 mag $\leq K_S \leq$ 14 mag. We find no background stars in this region, so accidental misclassification of companions as background stars is not an issue here.

[5] In this section we denote the *observed* quantities with a star as a subscript. For example, R denotes the substellar-to-stellar companion ratio (including all brown dwarfs), while $R_\star$ indicates the *observed* substellar-to-stellar companion ratio, including only the brown dwarfs brighter than $K_S = 14$ mag.

Table 8. The observed and expected number of brown dwarfs with $1'' \leq \rho \leq 4''$ and $12 \leq K_S \leq 14$ mag for the sample of 199 target stars. The left columns shows the various models for which we simulated observations. Each model has a semi-major axis distribution $f_a(a) \propto a^{-1}$ with $15\ R_\odot \leq a \leq 5 \times 10^6\ R_\odot$, and a multiplicity fraction of $F_M = 100\%$. Columns 3 and 4 show for a survey of intermediate mass stars (late-B and A stars; $1.4\ M_\odot < M < 7.7\ M_\odot$) the expected number of brown dwarfs $N_{\star,\rm BD,IM}$ and the substellar-to-stellar companion ratio $R_{\star,\rm IM}$, both with 1σ errors. By comparing the predicted values of $N_{\star,\rm BD,IM}$ and $R_{\star,\rm IM}$ with the observations, we can exclude models 1, 2, and 4. In Kouwenhoven et al. (2005) we exclude random pairing from the Preibisch mass distribution (models 1–3) since these models are inconsistent with the observed mass ratio distribution of stellar companions. We additionally list the values $N_{\star,\rm BD,LM}$ and $R_{\star,\rm LM}$ that are expected for a survey amongst 199 low-mass stars ($0.3\ M_\odot < M < 1.4\ M_\odot$) in Cols. 5 and 6. For models with $F_M < 100\%$ the expected number of brown dwarfs reduces to $F_M \times N_{\star,\rm BD}$, while R remains unchanged. Models with a smaller semi-major axis range and models with the log-normal period distribution found by Duquennoy & Mayor (1991) have a larger expected value of $N_{\star,\rm BD,IM}$, $N_{\star,\rm BD,LM}$. Under the assumption that companion mass and semi-major axis are uncorrelated, the values of $R_{\star,\rm IM}$ and $R_{\star,\rm LM}$ are equal to those listed above, if the log-normal period distribution is chosen.

#	Model	$N_{\star,\rm BD,IM}$	$R_{\star,\rm IM}$	$N_{\star,\rm BD,LM}$	$R_{\star,\rm LM}$
0	ADONIS/NACO observations	1 ± 1	0.036 ± 0.036	unknown	unknown
1	extended Preibisch MF, $\alpha = -0.9$, random pairing	5.50 ± 0.48	0.34 ± 0.03	7.19 ± 0.17	0.50 ± 0.01
2	extended Preibisch MF, $\alpha = -0.3$, random pairing	4.50 ± 0.41	0.24 ± 0.03	5.08 ± 0.13	0.30 ± 0.01
3	extended Preibisch MF, $\alpha = +2.5$, random pairing	1.07 ± 0.18	0.05 ± 0.01	1.42 ± 0.07	0.07 ± 0.01
4	Salpeter MF, random pairing	15.31 ± 2.79	6.00 ± 2.90	17.18 ± 0.88	3.95 ± 0.45
5	extended Preibisch MF, $\alpha = -0.9$, $f_q(q) \propto q^{-0.33}$	0.72 ± 0.24	0.04 ± 0.01	3.42 ± 0.14	0.18 ± 0.01
6	extended Preibisch MF, $\alpha = -0.3$, $f_q(q) \propto q^{-0.33}$	0.71 ± 0.22	0.04 ± 0.01	3.35 ± 0.14	0.18 ± 0.01
7	extended Preibisch MF, $\alpha = +2.5$, $f_q(q) \propto q^{-0.33}$	1.19 ± 0.27	0.06 ± 0.01	3.30 ± 0.13	0.18 ± 0.01
8	Salpeter MF, $f_q(q) \propto q^{-0.33}$	1.00 ± 0.57	0.05 ± 0.02	3.70 ± 0.57	0.20 ± 0.03

or from the the extended Preibisch mass distribution

$$f_{\rm M}(M) = \frac{{\rm d}M}{{\rm d}N} \propto \begin{cases} M^{\alpha} & \text{for} \quad 0.02 \leq M/M_\odot < 0.08 \\ M^{-0.9} & \text{for} \quad 0.08 \leq M/M_\odot < 0.6 \\ M^{-2.8} & \text{for} \quad 0.6 \leq M/M_\odot < 2 \\ M^{-2.6} & \text{for} \quad 2 \leq M/M_\odot < 20. \end{cases} \quad (7)$$

The extended Preibisch mass distribution (see Kouwenhoven et al. 2005) is based on the study by Preibisch et al. (2002), who derived $f_{\rm M}(M)$ with $M > 0.1\ M_\odot$ for the US subgroup of Sco OB2. Since our current knowledge about the brown dwarf population in OB associations (particularly Sco OB2) is incomplete (e.g., Table 2 in Preibisch et al. 2003) we simulate associations with three different slopes for the mass distribution in the brown dwarf regime. We extend the Preibisch mass distribution down to $0.02\ M_\odot$ with $\alpha = -0.9$, $\alpha = -0.3$, or $\alpha = +2.5$. The mass distribution with $\alpha = -0.9$ has the same slope in the brown dwarf regime as for the low-mass stars. The simulations with $\alpha = -0.3$ and $\alpha = +2.5$ bracket the values for α that are observed in various clusters and the field star population (see Preibisch et al. 2003, for a summary). The companion mass is obtained via randomly pairing the binary components from the mass distribution or via a mass ratio distribution of the form $f_q(q) \propto q^{-0.33}$ with $0 < q < 1$ and the requirement that any companion has a mass larger than $0.02\ M_\odot$. The latter mass ratio distribution was derived from the observed mass ratio distribution in our ADONIS survey (Kouwenhoven et al. 2005). For the models with random pairing, the primary star and companion mass are drawn independently from the mass distribution, and switched, if necessary, so that the primary is the most massive star.

Each simulated association consists of 100 000 binaries, has a distance of 130 pc and a homogeneous density distribution with a radius of 20 pc, properties similar to those of the subgroups in Sco OB2. We assume a thermal eccentricity distribution and a semi-major axis distribution of the form $f_a(a) \propto a^{-1}$, which is equivalent to $f_{\log a}(\log a) = \text{constant}$ (Öpiks law). The lower limit of a is set to $15\ R_\odot$. The upper limit is set to $5 \times 10^6\ R_\odot \approx 0.1$ pc, the separation of the widest observed binaries in the Galactic disk (e.g., Close et al. 1990; Chanamé & Gould 2004).

Table 8 lists for eight models the predicted value of $N_{\star,\rm BD}$, the expected number of brown dwarfs with $1'' \leq \rho \leq 4''$ and $12 \leq K_S \leq 14$ mag, normalized to a sample of 199 stars. The table also lists $R_\star$, the ratio between the number of brown dwarf companions with $K_S \leq 14$ mag and the number of stellar companions in the separation range $1'' - 4''$. Table 9 lists $N_{\rm BD}$ (the intrinsic number of brown dwarfs with $1'' \leq \rho \leq 4''$), and corresponding ratio R. In this table *all* companions are taken into account, including those with $K_S > 14$ mag. The values in Table 8 can be compared directly with the observations, while those in Table 9 represent the intrinsic properties of each association model. A brown dwarf with $K_S = 14$ mag in the US subgroup has a mass of less than $0.02\ M_\odot$ ($21\ M_{\rm J}$), and a brown dwarf with a similar brightness in the UCL and LCC subgroup has a mass of $\sim 0.038\ M_\odot$ ($40\ M_{\rm J}$).

Table 9. The observed and expected number of brown dwarfs with $1'' \leq \rho \leq 4''$ for the sample of 199 target stars. In this table we show the results for the full brown dwarf mass range ($0.02\ M_\odot \leq M \leq 0.08\ M_\odot$), unlike in Table 8, where we show the results for the brown dwarfs restricted to $12 \leq K_S \leq 14$ mag.

#	$N_{\rm BD,IM}$	$R_{\rm IM}$	$N_{\rm BD,LM}$	$R_{\rm LM}$
0	unknown	unknown	unknown	unknown
1	6.68 ± 0.53	0.44 ± 0.04	8.50 ± 0.18	0.65 ± 0.02
2	5.46 ± 0.45	0.31 ± 0.03	6.42 ± 0.15	0.42 ± 0.01
3	2.01 ± 0.25	0.10 ± 0.01	2.65 ± 0.09	0.14 ± 0.01
4	15.82 ± 2.84	7.75 ± 4.12	18.26 ± 0.91	5.60 ± 0.72
5	1.20 ± 0.31	0.06 ± 0.02	4.26 ± 0.16	0.24 ± 0.01
6	1.13 ± 0.28	0.06 ± 0.02	4.30 ± 0.16	0.25 ± 0.01
7	1.42 ± 0.29	0.07 ± 0.01	4.18 ± 0.14	0.24 ± 0.01
8	1.19 ± 0.63	0.06 ± 0.03	5.02 ± 0.66	0.30 ± 0.04

The definition of the brown dwarf desert given in the beginning of this section is generally used for binarity studies of late-type stars. In our study the primaries are intermediate mass stars, allowing companion stars over a larger mass range than for low mass primaries. This naturally leads to lower values of $N_{\rm BD}$ and R. We therefore also list the results for a simulated survey of 199 low mass stars. Tables 8 and 9 show that indeed the expected values $N_{\rm BD}$ and R for low-mass stars are higher than those for intermediate-mass stars by ~30% for the random pairing models, and by ~250% for the models with $f_q(q) \propto q^{-0.33}$.

A multiplicity fraction of $F_M = 100\%$ is assumed in each model. For A and late B members of Sco OB2 the *observed*

multiplicity fraction $F_{\rm M}$ is ≈50% (Kouwenhoven et al. 2005). This is a lower limit of the *true* multiplicity fraction due to the presence of unresolved companions, and hence we have $50\% \lesssim F_{\rm M} \leq 100\%$. For a multiplicity fraction smaller than 100%, the expected number of brown dwarfs is given by $F_{\rm M} \times N_{\star,\rm BD}$, while the values of R remain unchanged. In each model we adopted Öpiks law, with $15\ R_\odot \leq a \leq 5 \times 10^6\ R_\odot$. In reality, the upper limit for a may be smaller, as Sco OB2 is an expanding association (Blaauw 1964; Brown et al. 1999). If this is true, the values for $N_{\star,\rm BD}$ are underpredicted, as less companions are expected to have very large separations. Furthermore, instead of Öpiks law, it may also be possible that the log-normal period distribution found by Duquennoy & Mayor (1991) holds. For a model with Öpiks law at a distance of 130 pc, 11% of the companions have separations between 1″–4″, while for a model with the log-normal period distribution, 13% of the companions have separations between 1″–4″. If the log-normal period distribution holds, the values for $N_{\star,\rm BD}$ in Tables 8 and 9 are underpredicted. The value of R (and $R_\star$) does not change for the possible adaptations described here, under the assumption that the stellar and substellar companions have the same semi-major axis (or period) distribution.

Table 8 shows that the models with $f_q(q) \propto q^{-0.33}$ are in good agreement with our observations for any value of α. The reason for this is that $N_{\star,\rm BD,IM}$ and $R_{\star,\rm IM}$ are independent of α for these models, as only the primary is chosen from the mass distribution. For the models with random pairing, the two components of each binary system are *independently* chosen from the mass distribution. Only those models with a turnover in the mass distribution in the brown dwarf regime are consistent with the observations (for a multiplicity fraction of $0.5 \lesssim F_{\rm M} \leq 1$). However, in Kouwenhoven et al. (2005) we excluded random pairing by studying the observed mass ratio distribution for stellar companions. The remaining models that are consistent with our observations have an extended Preibisch mass distribution and a mass ratio distribution of the form $f_q(q) \propto q^{-0.33}$. Although this distribution is peaked to low values of q, the number of brown dwarf companions is significantly smaller than the number of stellar companions. For example, for a sample of binaries with a primary mass of 3 $M_\odot$, the substellar-to-stellar companion mass ratio R (see Eq. (5)) resulting from $f_q(q) \propto q^{-0.33}$ is given by

$$R = \frac{\int_{0.02/3}^{0.08/3} f_q(q)\,\mathrm{d}q}{\int_{0.08/3}^{1} f_q(q)\,\mathrm{d}q} = \frac{\left[\, q^{0.67} \,\right]_{0.02/3}^{0.08/3}}{\left[\, q^{0.67} \,\right]_{0.08/3}^{1}} = 0.059. \quad (8)$$

Figure 9 further illustrates that a small value for R is expected among binaries with an intermediate-mass or solar-type primary, even if $f_q(q)$ is strongly peaked to low values of q. Among primaries with a mass of 1 $M_\odot$ and 3 $M_\odot$, this fraction is ∼14% and ∼6%, respectively. For this mass ratio distribution, the number of brown dwarf companions is significantly smaller than the number of stellar companions, even if observational biases are not taken into account. If binary formation truly results in a mass ratio distribution similar to $f_q(q) \propto q^{-0.33}$, the brown dwarf desert (in terms of the "deficit" of brown dwarf companions relative to stellar companions) is a natural outcome of the star forming process for intermediate mass stars.

The observed number of brown dwarfs (with 12 mag $\leq K_{\rm S} \leq$ 14 mag) is $N_{\star,\rm BD,IM} = 1 \pm 1$. After correction for unseen low-mass brown dwarfs (with $K_{\rm S} > 14$ mag) this translates to $N_{\rm BD,IM} = 1.6 \pm 1.6$ brown dwarfs (cf. Tables 8 and 9). If we assume a semi-major axis distribution of the form $f_a(a) \propto a^{-1}$ with $15\ R_\odot < a < 5 \times 10^6\ R_\odot$ and a distance of 130 pc, we expect ∼11% of the companions to be in the angular separation range 1″–4″. Assuming that companion mass and semi-major axis are uncorrelated, this also means that 11% of the brown dwarfs are in this range. Extrapolation gives an estimate of $(1.6 \pm 1.6)/0.11 = 14.5 \pm 14.5$ brown dwarf companions around the 199 target stars, or a brown dwarf companion fraction of 7.3 ± 7.3% for intermediate mass stars in Sco OB2. On the other hand, if we assume the log-normal period distribution found by Duquennoy & Mayor (1991), we find a corresponding brown dwarf companion fraction of 6.2 ± 6.2% (for a model binary fraction of 100%). Note that if a mass ratio distribution $f_q(q)$ is adopted, these values are independent of the slope α of the mass distribution in the brown dwarf regime.

McCarthy & Zuckerman (2004) find a companion frequency of 0.7 ± 0.7% for brown dwarf companions ($M > 30\ M_{\rm J}$) to F, G, K, and M stars in the separation range 120–1200 AU. Assuming a semi-major axis distribution of the form $f_a(a) \propto a^{-1}$, our brown dwarf companion frequency of 0.5 ± 0.5% ($M \gtrsim 30\ M_{\rm J}$) for the range 130–520 AU translates to a value of 0.83 ± 0.83% for the range 120–1200 AU, which is in good agreement with the frequency found by McCarthy & Zuckerman (2004). This "extrapolated" brown dwarf companion frequency may underestimate the true value, if the brown dwarf desert does not exist at larger separations (which may be the case for low-mass stars in the solar neighbourhood; e.g., Gizis et al. 2001).

6.3. The origin of the brown dwarf desert

Most stars are formed and reside in binary or multiple stellar systems. Knowledge about binary and multiple systems in young stellar groupings is of fundamental importance for our understanding of the star formation process. The formation of brown dwarfs and the dearth of brown dwarf companions has attained much interest over the last decade. Theories have been developed, explaining the existence of the brown dwarf desert using migration (Armitage & Bonnell 2002, most effective at $a \lesssim 5$ AU) or ejection (Reipurth & Clarke 2001) of brown dwarfs. The most popular theory that explains the brown dwarf desert is the *embryo ejection scenario*. This scenario predicts ejection of brown dwarfs soon after their formation by dynamical interactions in unstable multiple systems (Reipurth & Clarke 2001). Hydrodynamical calculations (e.g., Bate et al. 2003) suggest that star formation is a highly dynamic and chaotic process. Brown dwarfs are ejected during or soon after their formation. In this theory brown dwarfs can be seen as failed stellar companions.

In the section above we have shown that the small number of brown dwarfs among A and late-B members of Sco OB2 can be explained with an extrapolation of the mass ratio distribution for stellar companions into the brown dwarf regime. There is thus no need for a mechanism to remove brown dwarfs. On the other hand, the embryo ejection scenario predicts that (at least a fraction of) the free-floating brown dwarfs in Sco OB2 have been formed as companions to association members. Below, we study the consequences in the case that embryo ejection has affected the binary population, making use of the detection of 28 free-floating brown dwarfs in Upper Scorpius by Martín et al. (2004). Under the assumption that this is what happened, we roughly estimate the number of primordial binaries with an A or late-B primary and a brown dwarf companion. For comparison between model predictions and observations we consider only those companions with an angular separation $1'' \leq \rho \leq 4''$ and

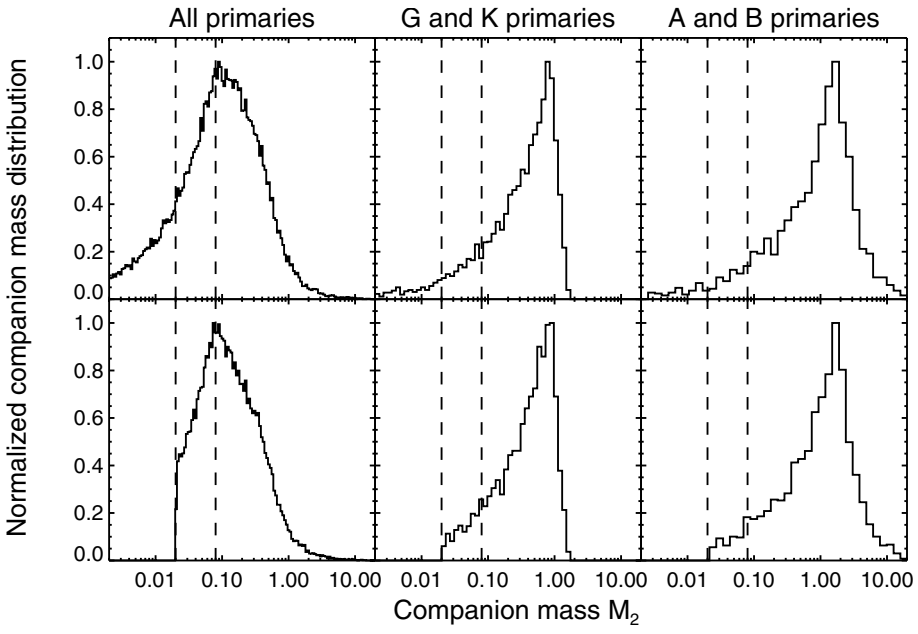

Fig. 9. The companion mass distribution $f_{M_2}(M_2)$ for a simulated association. In each panel we show the distribution $f_{M_2}(M_2)$ of an association consisting of 50 000 binaries for which the primary mass distribution is given by Eq. (7). From left to right, the panels show the distribution of companion mass in all binaries with stellar primaries, for those of G and K primaries, and for those of A and B primaries, respectively. In the top panels we adopted a mass ratio distribution $f_q(q) \propto q^{-0.33}$ with $0 < q \leq 1$. In the bottom panels we adopt the same distribution, but with the additional constraint that $M_2 \geq 0.02\ M_\odot$. The brown dwarf regime is indicated with the dashed lines. This figure shows that, even though the mass ratio distribution is strongly peaked to low values of q, the substellar-to-stellar companion ratio among intermediate- and high-mass stars is very low.

$K_S < 14$ mag, for which our ADONIS and NACO observations are complete.

Martín et al. (2004) present a sample of 104 candidate very low mass members, based on DENIS IJK photometry, in a region of 60 square degrees in US. The authors report spectroscopic observations of 40 of these candidates and show that 28 are indeed strong candidate members of the US subgroup. Under the assumption that Martín et al. (2004) randomly selected their 40 observed targets out of the sample of 104 candidates, we estimate the total number of brown dwarfs in US to be 73 ± 14 in the 60 square degrees region in US. The projected area of the three subgroups of Sco OB2 is approximately 960 square degrees, which gives us an estimate of 1165 ± 221 free-floating brown dwarfs in Sco OB2.

For our estimate of the number of primordial binaries we assume that all free-floating brown dwarfs were once companions. The number of systems with an A or late-B primary constitutes a small fraction $F_{\rm IM}$ of the total number of binaries, depending on the mass distribution (see Table 10). Assuming a primordial semi-major axis distribution of the form $f_a(a) \propto a^{-1}$ with $15\ R_\odot < a < 5 \times 10^6\ R_\odot$, about 11% of the brown dwarf companions are in the angular separation range $1'' \leq \rho \leq 4''$.

For each model in Table 10 we calculate how many of the 1165 ± 221 free-floating have the properties $1'' \leq \rho \leq 4''$ and $K_S < 14$ mag, and obtain the contribution $N_{\rm BD,IM,i} = F_{1''-4''} \times F_{\rm IM} \times (1165 \pm 221)$ of the free-floating brown dwarfs found by Martín et al. (2004) to the number of primordial binaries in Sco OB2 with A and late-B primaries and brown dwarf companions in the angular separation range $1'' \leq \rho \leq 4''$. We estimate the total number of primordial brown dwarf companions $N_{\rm BD,IM,i,total}$ with $1'' \leq \rho \leq 4''$ of A and late-B primaries by adding the observed number of brown dwarf companions, corrected for unseen companions with $K_S > 14$ mag (i.e., 1.67 ± 1.67).

We have assumed that all free-floating brown dwarfs were once companion stars, and therefore obtained upper limits for $N_{\rm BD,IM,i,total}$. By comparing $N_{\rm BD,IM}$ in Table 9 with $N_{\rm BD,IM,i,total}$ in Table 10 we can derive which primordial mass and mass ratio distributions are consistent with the predictions. As not necessarily all free-floating brown dwarfs have their origin in a binary system, all models with $N_{\rm BD,IM} \lesssim N_{\rm BD,IM,i,total}$ are consistent with the predictions (i.e., the *current* number of brown dwarf companions should be less or equal to the *primordial* number of brown dwarf companions). A comparison shows that all models are consistent, except model 4 (random pairing from the Salpeter mass distribution). Under the hypothesis that embryo ejection has affected Sco OB2, the current mass ratio distribution is slightly shallower than the primordial mass ratio distribution, due to the ejection of brown dwarf companions. The above derivation gave an estimate of the number of primordial binaries with brown dwarf companions, under the assumption that the origin of the free-floating brown dwarfs in Sco OB2 can be explained with the embryo ejection scenario. With our observations we cannot exclude firmly that this happened for several of the free-floating brown dwarfs.

Table 10. An estimate of the number of *primordial* binaries in Sco OB2 with A and late-B primaries and brown dwarf companions (with $0.02\ M_\odot \leq M \leq 0.08\ M_\odot$) in the angular separation range $1'' \leq \rho \leq 4''$. Columns 1 and 2 list the model number (cf. Table 8), and the fraction of binaries with angular separation $1'' \leq \rho \leq 4''$ (assuming Öpik's law). Column 3 lists the fraction $F_{\rm IM}$ of primaries in the simulated association that is of type A or late-B. Column 4 shows the contribution of brown dwarf companions in Sco OB2 with A and late-B primaries in the angular separation range $1'' \leq \rho \leq 4''$, inferred from the 28 free-floating brown dwarfs in Sco OB2 found by Martín et al. (2004), assuming that *all* brown dwarfs were formed as companions. Column 5 shows the total number of primordial brown dwarf companions with $1'' \leq \rho \leq 4''$ and A or late-B primaries, with the observed brown dwarf companions (corrected for unseen brown dwarfs with $K > 14$ mag) included. The values of $N_{\rm BD,IM,i,total}$ are upper limits, as it is likely that not *all* free-floating brown dwarfs were formed as companions.

#	$F_{1''-4''}$ (%)	$F_{\rm IM}$ (%)	$N_{\rm BD,IM,i}$	$N_{\rm BD,IM,i,total}$
1	10.9	4.93	6.26 ± 1.19	7.93 ± 2.05
2	10.9	5.34	6.78 ± 1.29	8.45 ± 2.11
3	10.9	6.33	8.04 ± 1.52	9.71 ± 2.26
4	10.9	0.40	0.51 ± 0.10	2.18 ± 1.67
5	10.9	2.45	3.11 ± 0.59	4.78 ± 1.77
6	10.9	2.70	3.43 ± 0.65	5.10 ± 1.79
7	10.9	3.19	4.05 ± 0.77	5.72 ± 1.84
8	10.9	0.20	0.25 ± 0.05	1.92 ± 1.67

However, if binary formation would result in a mass ratio distribution similar to $f_q(q) \propto q^{-0.33}$, the "brown dwarf desert", if defined as a deficit of brown dwarf companions relative to stellar companions, would be a *natural outcome of star formation*. The embryo ejection scenario is not necessary to explain the small observed brown dwarf companion fraction in this case.

7. Binarity and multiplicity in Sco OB2

In Kouwenhoven et al. (2005) we provided a census on binarity in Sco OB2, consisting of all available data on visual, spectroscopic, eclipsing, and astrometric binaries and multiples. In Table 1 we present an update on the binary statistics in Sco OB2. The statistics have been updated with the new results presented in this paper, as well as with the binaries recently discovered by Nitschelm (2004), Jilinski et al. (2006), and Chen et al. (2006).

The multiple system fraction $F_{\rm M}$, the non-single star fraction $F_{\rm NS}$, and companion star fraction $F_{\rm C}$ are defined as:

$$F_{\rm M} = (B + T + \ldots) \,/\, (S + B + T + \ldots); \quad (9)$$

$$F_{\rm NS} = (2B + 3T + \ldots) \,/\, (S + 2B + 3T + \ldots); \quad (10)$$

$$F_{\rm C} = (B + 2T + \ldots) \,/\, (S + B + T + \ldots), \quad (11)$$

where S, B, and T denote the number of single systems, binary systems and triple systems in the association. In the Sco OB2 association at least 40% of the systems are multiple. Of the individual stars at least 60% is part of a multiple system. Each system contains on average $F_{\rm C} \approx 0.5$ known companion stars. The updated values of $F_{\rm M}$, $F_{\rm NS}$, and $F_{\rm C}$ are slightly larger than the values mentioned in Kouwenhoven et al. (2005), respectively. Note that these frequencies are lower limits due to the presence of undiscovered companion stars.

8. Conclusions

We have carried out near-infrared $JHK_{\rm S}$ observations of 22 A and late-B stars in the Sco OB2 association. The observations were performed with the NAOS/CONICA system at the ESO Very Large Telescope at Paranal, Chile. The observations resulted from a follow-up program of our previous work (Kouwenhoven et al. 2005), in which we surveyed 199 A and late-B Sco OB2 members for binarity with ADONIS. The data were obtained with the goal of (1) determining the validity of the $K_{\rm S} = 12$ mag criterion we used in our ADONIS survey to separate companions and background stars, (2) studying the behaviour of the companion mass distribution in the low-mass regime, and (3) searching for additional companion stars. We have included in our analysis the multi-color observations of 9 targets observed with ADONIS. In our ADONIS survey, these targets were analyzed using their $K_{\rm S}$ magnitude only. The main results of our study are:

- We detect 72 secondaries around the 31 target stars in our analysis. By comparing the near-infrared colors with the isochrones in the color–magnitude diagram, we find 25 confirmed companion stars, 12 candidate companion stars, and 35 background stars.
- For most objects in our ADONIS survey (Kouwenhoven et al. 2005) only the $K_{\rm S}$ magnitude was available. We used a magnitude criterion to separate companion stars ($K_{\rm S} <$ 12 mag) and background stars ($K_{\rm S} >$ 12 mag). With our analysis of the 22 NACO targets and 9 ADONIS targets with multi-color observations, we estimate the accuracy of the $K_{\rm S} = 12$ mag criterion. We find that the $K_{\rm S} = 12$ mag criterion is a very useful tool, correctly classifying the secondaries in ~80% of the cases.
- We report two candidate brown dwarf companions of HIP 81972. >From their near-infrared magnitudes we infer masses of 32 $M_{\rm J}$ and 63 $M_{\rm J}$. The objects are located at an angular separation of 7.92″ (1500 AU) and 2.79″ (520 AU) from HIP 81972, respectively. Follow-up spectroscopy is necessary to determine the true nature of these secondaries. Although we are sensitive (but incomplete) to massive planets, we classify the faintest secondaries as background stars (irrespective of their location in the color–magnitude diagram), because of isochronal uncertainty and the large number of faint background stars.
- In our combined survey of 199 A and late-B members of Sco OB2 we detect one confirmed companion star with 12 mag $\leq K_{\rm S} \leq$ 14 mag in the angular separation range 1″–4″. In this region we detect no other secondary, while both the ADONIS and NACO observations are complete. This indicates a very low frequency of brown dwarf companions in the separation range 130–520 AU for late-B and A type stars in Sco OB2.
- Our results are in good agreement with a mass ratio distribution of the form $f_q(q) \propto q^{-0.33}$. We find a brown dwarf companion fraction (for $M \gtrsim 30\ M_{\rm J}$) of $0.5 \pm 0.5\%$ for A and late-B stars in Sco OB2. After correction for unseen faint companions ($M \lesssim 30\ M_{\rm J}$), we estimate a substellar-to-stellar companion ratio of $R = 0.06 \pm 0.02$.

The number of brown dwarfs among A and late-B members of Sco OB2 is consistent with an extrapolation of the (stellar) companion mass distribution into the brown dwarf regime, suggesting that the formation mechanism for stars and brown dwarfs is the same. The embryo ejection mechanism does not need to be invoked to explain the small number of brown dwarf companions among intermediate mass stars in Sco OB2.

Acknowledgements. We thank ESO and the Paranal Observatory staff for efficiently conducting the Service-Mode observations and for their support. We thank Simon Portegies Zwart and the anonymous referee for their constructive criticism, which helped to substantially improve the paper. This publication makes use of data products from the Two Micron All Sky Survey, which is a joint project of the University of Massachusetts and the Infrared Processing and Analysis Center/California Institute of Technology, funded by the National Aeronautics and Space Administration and the National Science Foundation. This research is supported by NWO under project number 614.041.006.

References

Armitage, P. J., & Bonnell, I. A. 2002, MNRAS, 330, L11
Bate, M. R., Bonnell, I. A., & Bromm, V. 2003, MNRAS, 339, 577
Blaauw, A. 1964, ARA&A, 2, 213
Blaauw, A. 1991, in NATO ASIC Proc. 342: The Physics of Star Formation and Early Stellar Evolution, 125
Brown, A. 2001, Astron. Nachr., 322, 43
Brown, A. G. A., Arenou, F., van Leeuwen, F., Lindegren, L., & Luri, X. 1997, The First Results of Hipparcos and Tycho, 23rd meeting of the IAU, Joint Discussion 14, 25 August 1997, Kyoto, Japan, meeting abstract, 14
Brown, A. G. A., Blaauw, A., Hoogerwerf, R., de Bruijne, J. H. J., & de Zeeuw, P. T. 1999, in NATO ASIC Proc. 540: The Origin of Stars and Planetary Systems, ed. C. J. Lada, & N. D. Kylafis, 411
Chabrier, G., Baraffe, I., Allard, F., & Hauschildt, P. 2000, ApJ, 542, 464
Chabrier, G., Baraffe, I., Allard, F., & Hauschildt, P. H. 2005, in Resolved Stellar Populations, ASP Conf. Ser., ed. Valls-Gabaud & Chavez
Chanamé, J., & Gould, A. 2004, ApJ, 601, 289
Chen, X. P., Henning, T., van Boekel, R., & Grady, C. A. 2006, A&A, 445, 331
Close, L. M., Richer, H. B., & Crabtree, D. R. 1990, AJ, 100, 1968
Cox, A. N. 2000, Allen's astrophysical quantities, ed. Arthur N. Cox (New York: Springer), 2000
Cunha, K., & Lambert, D. L. 1994, ApJ, 426, 170

Cutri, R. M., Skrutskie, M. F., van Dyk, S., et al. 2003, VizieR Online Data Catalog, 2246
de Bruijne, J. H. J. 1999, MNRAS, 310, 585
de Geus, E. J., de Zeeuw, P. T., & Lub, J. 1989, A&A, 216, 44
de Zeeuw, P. T., Hoogerwerf, R., de Bruijne, J. H. J., Brown, A. G. A., & Blaauw, A. 1999, AJ, 117, 354
Devillard, N. 1997, The Messenger, 87, 19
Diolaiti, E., Bendinelli, O., Bonaccini, D., et al. 2000, A&AS, 147, 335
Duquennoy, A., & Mayor, M. 1991, A&A, 248, 485
Girardi, L., Bertelli, G., Bressan, A., et al. 2002, A&A, 391, 195
Gizis, J. E., Kirkpatrick, J. D., Burgasser, A., et al. 2001, ApJ, 551, L163
Huélamo, N., Brandner, W., Brown, A. G. A., Neuhäuser, R., & Zinnecker, H. 2001, A&A, 373, 657
Jilinski, E., Daflon, S., Cunha, K., & de La Reza, R. 2006, A&A, 448, 1001
Kouwenhoven, M. B. N. 2006, Ph.D. Thesis, University of Amsterdam [arXiv:astro-ph/0610792]
Kouwenhoven, M. B. N., Brown, A. G. A., Zinnecker, H., Kaper, L., & Portegies Zwart, S. F. 2005, A&A, 430, 137
Lenzen, R., Hofmann, R., Bizenberger, P., & Tusche, A. 1998, in Infrared Astronomical Instrumentation, Proc. SPIE, 3354, 606, ed. A. M. Fowler
Mamajek, E. E., Meyer, M. R., & Liebert, J. 2002, AJ, 124, 1670
Martín, E. L., Delfosse, X., & Guieu, S. 2004, AJ, 127, 449
McCarthy, C. & Zuckerman, B. 2004, AJ, 127, 2871
Nitschelm, C. 2004, in Spectroscopically and Spatially Resolving the Components of the Close Binary Stars, ed. R.W. Hidlitch, H. Hensberge, & K. Pavlovski, ASP Conf. Ser., 318, 291
Palla, F., & Stahler, S.W. 1999, ApJ, 525, 772
Persson, S. E., Murphy, D. C., Krzeminski, W., Roth, M., & Rieke, M. J. 1998, AJ, 116, 2475
Portegies Zwart, S. F., McMillan, S. L. W., Hut, P., & Makino, J. 2001, MNRAS, 321, 199
Poveda, A., Allen, C., & Parrao, L. 1982, ApJ, 258, 589
Preibisch, T., Brown, A. G. A., Bridges, T., Guenther, E., & Zinnecker, H. 2002, AJ, 124, 404
Preibisch, T., Stanke, T., & Zinnecker, H. 2003, A&A, 409, 147
Press, W. H., Teukolsky, S. A., Vetterling, W. T., & Flannery, B. P. 1992, Numerical recipes in FORTRAN. The art of scientific computing, 2nd edn. (Cambridge: University Press)
Reipurth, B. & Clarke, C. 2001, AJ, 122, 432
Robin, A. C., Reylé, C., Derrière, S., & Picaud, S. 2003, A&A, 409, 523
Rousset, G., Lacombe, F., Puget, P., et al. 2000, in Adaptive Optical Systems Technology, ed. P. L. Wizinowich, Proc. SPIE, 4007, 72
Shatsky, N., & Tokovinin, A. 2002, A&A, 382, 92
Siess, L., Dufour, E., & Forestini, M. 2000, A&A, 358, 593
Worley, C. E., & Douglass, G. G. 1997, A&AS, 125, 523

Online Material

Appendix A: Results of the NAOS/CONICA survey

Table A.1. Results from our multi-color binarity study among 22 Sco OB2 member stars observed with NACO (*top part of the table*) and the subset of 9 members with multi-color observations in in the ADONIS survey (*bottom part of the table*). The columns show the *Hipparcos* number (for the targets) and the secondary designation, the J, H, and K_S magnitudes, the angular separation, and the position angle (measured from North to East). Lower limits to the magnitudes are given if an object is not detected in the NACO survey, unless the ADONIS measurement was available (marked with a ⋆). Entries marked with ⋆⋆ have no available measurement, e.g., because the object is not in the field of view for that filter. For each primary and companion star we list the absolute JHK_S magnitudes and the mass in Cols. 7−10. We additionally provide absolute magnitudes and a mass estimate for the candidate companions, *under the assumption* that these are indeed companions. We stress that a significant number of the candidate companions may actually be background stars. The 11th column lists the status of the object (p = primary, c = confirmed companion star, nc = new confirmed companion star, ? = candidate companion star; b = background star). The last column provides additional remarks. A remark "J", "H", or "K" means that the secondary flux in this filter was obtained from the image obtained *without* the NDF, using the PSF from the corresponding image that was obtained *with* NDF (see Sect. 2.4). If the secondary status was obtained without color information, an exclamation mark is placed in the last column. The results for the 9 targets with multi-color information in the ADONIS survey are marked with "ADO".

Star	J	H	K_S	ρ	PA	M_J	M_H	M_{K_S}	Mass	Status	Remarks
	mag	mag	mag	arcsec	deg	mag	mag	mag	$M_\odot$		
HIP 59502	6.83	6.83	6.87			1.86	1.87	1.91	1.80	p	
HIP 59502 -1	12.35	11.83	11.64	2.94	26.39	7.39	6.86	6.68	0.14	c	
HIP 59502 -2	>15.22	15.26	15.37	4.76	101.87					b	HK
HIP 59502 -3	⋆⋆	⋆⋆	13.69	9.02	309.01					b	K!
HIP 60851	6.03	6.06	6.06			0.94	0.97	0.97	2.63	p	
HIP 60851 -1	12.81	11.62	11.46	2.07	45.30					b	J
HIP 60851 -2	>13.33	11.68	11.29	6.89	180.38					b	
HIP 60851 -3	>13.33	13.63	13.69	8.16	231.46	(>8.24)	(8.54)	(8.60)	(0.04)	?	HK
HIP 60851 -4	>13.33	14.82	14.80	1.61	280.38					b	HK
HIP 60851 -5	>13.33	15.53	14.97	8.19	69.19					b	HK
HIP 60851 -6	>13.33	15.83	⋆⋆	7.65	153.67					b	H!
HIP 60851 -7	>13.33	16.67	⋆⋆	7.47	287.03					b	H!
HIP 60851 -8	>13.33	16.87	16.97	5.45	76.38					b	HK
HIP 61265	7.49	7.51	7.46			1.85	1.87	1.81	1.82	p	
HIP 61265 -1	11.98	11.66	11.38	2.51	67.15	(6.34)	(6.02)	(5.74)	(0.27)	?	J
HIP 61265 -2	15.13	14.96	14.75	3.41	167.27					b	J
HIP 61265 -3	>15.71	16.30	15.29	7.00	24.46					b	
HIP 61265 -4	>15.71	16.80	16.28	6.60	31.84					b	
HIP 61265 -5	>15.71	>15.90	15.86	7.11	344.55					b	!
HIP 62026	6.28	6.32	6.31			1.09	1.12	1.11	2.45	p	
HIP 62026 -1	8.08	7.90	7.86	0.23	6.34	2.88	2.71	2.66	1.19	c	
HIP 63204	6.68	6.76	6.78			1.48	1.55	1.57	2.05	p	
HIP 63204 -1	8.72	7.85	7.50	1.87	47.44					b	
HIP 63204 -2	8.79	8.51	8.40	0.15	236.56	3.59	3.31	3.19	1.06	c	
HIP 67260	7.03	7.00	6.98			1.57	1.53	1.52	2.00	p	
HIP 67260 -1	8.88	8.46	8.36	0.42	229.46	3.42	2.99	2.90	1.10	c	
HIP 67260 -2	⋆⋆	14.04	14.10	1.23	355.65	(⋆⋆)	(8.57)	(8.63)	(0.04)	?	
HIP 67260 -3	15.84	14.83	14.67	2.33	77.25	(10.38)	(9.36)	(9.20)	(≈0.02)	?	JHK
HIP 67919	6.71	6.60	6.59			1.63	1.52	1.51	1.97	p	
HIP 67919 -1	9.98	9.38	9.10	0.69	296.56	4.89	4.30	4.02	0.75	c	
HIP 68532	7.16	7.08	7.02			1.67	1.59	1.53	1.95	p	
HIP 68532 -1	10.52	9.85	9.54	3.05	288.50	5.03	4.36	4.05	0.73	c	
HIP 68532 -2	11.38	10.94	10.63	3.18	291.92	5.89	5.45	5.14	0.39	c	
HIP 69113	6.17	6.30	6.37			0.02	0.15	0.22	3.87	p	
HIP 69113 -1	10.98	10.43	10.29	5.34	65.15	4.83	4.28	4.14	0.77	c	
HIP 69113 -2	11.27	10.45	10.30	5.52	67.17	5.12	4.29	4.15	0.72	c	
HIP 73937	6.11	6.21	6.23			0.65	0.75	0.77	2.94	p	
HIP 73937 -1	>8.40	8.46	8.37	0.24	190.58	>2.94	3.00	2.91	1.11	c	
HIP 73937 -2	>11.41	14.32	14.71	3.56	31.24					b	HK
HIP 78968	7.47	7.42	7.42			1.23	1.17	1.18	2.33	p	
HIP 78968 -1	14.96	14.51	14.26	2.78	322.13	(8.71)	(8.27)	(8.01)	(≈0.02)	?	JHK
HIP 79098	5.71	5.70	5.69			–0.02	–0.03	–0.04	4.30	p	
HIP 79098 -1	15.67	14.14	14.24	2.37	116.63					b	JK
HIP 79410	7.20	7.14	7.09			1.35	1.29	1.24	2.24	p	
HIP 79410 -1	15.94	15.12	14.93	3.24	340.93					b	J
HIP 79739	7.17	7.16	7.08			1.23	1.21	1.14	2.32	p	
HIP 79739 -1	12.28	11.52	11.23	0.96	118.33	6.34	5.58	5.29	0.16	c	
HIP 79771	7.33	7.26	7.10			1.39	1.31	1.15	2.14	p	
HIP 79771 -1	12.00	11.28	10.89	3.67	313.38	6.06	5.33	4.94	0.19	c	
HIP 79771 -2	12.39	11.79	11.42	0.44	128.59	6.44	5.85	5.47	0.13	nc	
HIP 80142	6.61	6.67	6.66			0.41	0.47	0.46	3.33	p	
HIP 80142 -1	12.01	10.59	9.51	9.23	216.16					b	J
HIP 80142 -2	16.64	15.88	⋆⋆	5.88	119.94	(10.44)	(9.68)	(⋆⋆)	(≈0.02)	?	HJ
HIP 80474	6.14	5.92	5.80			0.27	0.05	–0.07	3.78	p	

Table A.1. continued.

Star	J mag	H mag	K_S mag	ρ arcsec	PA deg	M_J mag	M_H mag	M_{K_S} mag	Mass $M_\odot$	Status	Remarks
HIP 80474 -1	12.06	12.34	10.79	4.85	206.36					b	*JHK*
HIP 80799	7.56	7.53	7.45			2.04	2.01	1.93	1.86	p	
HIP 80799 -1	10.60	10.04	9.80	2.94	205.02	5.08	4.51	4.27	0.34	c	
HIP 80896	7.67	7.53	7.44			2.11	1.97	1.88	1.81	p	
HIP 80896 -1	11.16	10.63	10.33	2.28	177.23	5.60	5.07	4.77	0.24	c	
HIP 81949	7.38	7.40	7.33			1.28	1.31	1.23	2.26	p	
HIP 81949 -1	15.73	14.11	13.28	3.91	88.47					b	
HIP 81949 -2	14.34	14.28	14.06	3.48	28.46					b	
HIP 81949 -3	>16.81	15.26	14.75	5.70	292.80					b	
HIP 81949 -4	>16.81	15.67	15.52	5.27	340.72	(>10.71)	(9.57)	(9.42)	(≈0.02)	?	
HIP 81949 -5	>16.81	16.52	>15.93	9.63	76.17					b	!
HIP 81949 -6	>16.81	15.62	14.82	6.26	239.37	(>10.71)	(9.52)	(8.73)	(≈0.02)	?	
HIP 81949 -7	>16.81	>16.84	15.59	11.72	40.80					b	!
HIP 81949 -8	>16.81	>16.84	16.75	4.16	236.05					b	!
HIP 81949 -9	>16.81	>16.84	16.83	3.86	105.30					b	!
HIP 81949 -10	>16.81	>16.84	17.10	2.38	48.01					b	!
HIP 81949 -11	>16.81	>16.84	17.15	8.05	96.11					b	!
HIP 81949 -12	>16.81	>16.84	17.34	8.13	36.64					b	!
HIP 81972	5.82	5.89	5.87			–0.56	–0.49	–0.51	4.92	p	
HIP 81972 -1	11.63	10.87	10.48	2.02	313.69	(5.25)	(4.49)	(4.10)	(0.67)	?	
HIP 81972 -2	11.30	10.97	10.61	7.02	258.81	(4.92)	(4.59)	(4.23)	(0.68)	?	
HIP 81972 -3	12.54	11.86	11.77	5.04	213.45	6.16	5.48	5.39	0.35	c	*J*
HIP 81972 -4	15.10	14.43	13.98	2.79	106.94	8.72	8.05	7.60	0.06	nc	*JHK*
HIP 81972 -5	16.11	15.63	15.26	7.92	229.27	9.73	9.25	8.88	≈0.03	nc	*JHK*
HIP 81972 -6	>16.58	16.25	>16.61	8.79	167.71					b	*H*!
HIP 81972 -7	>16.58	17.12	>16.61	3.58	33.65					b	*H*!
HIP 81972 -8	>16.58	17.28	>16.61	7.44	265.65					b	*H*!
HIP 83542	5.34	4.91	5.38			–1.26	–1.69	–1.22	1.10	p	
HIP 83542 -1	⋆⋆	9.72	9.90	8.86	196.21	(⋆⋆)	(3.12)	(3.30)	(0.91)	?	
HIP 83542 -2	>15.54	15.65	>12.13	9.84	156.45					b	*H*!
ADONIS targets with multi-color observations											
HIP 53701	6.30	6.37	6.48			0.79	0.86	0.97	2.84	p	ADO
HIP 53701 -1	9.05	8.76	8.86	3.88	75.81					b	ADO
HIP 53701 -2	13.06	12.93	13.04	6.57	120.05					b	ADO
HIP 76071	7.05	7.10	7.06			0.89	0.94	0.90	2.70	p	ADO
HIP 76071 -1	>11.25	11.28	10.87	0.69	40.85	>5.09	5.12	4.71	0.23	c	ADO
HIP 77911	6.67	6.71	6.68			0.81	0.85	0.82	2.80	p	ADO
HIP 77911 -1	12.68	12.20	11.84	7.96	279.25	6.82	6.34	5.98	0.09	c	ADO
HIP 78530	6.87	6.92	6.87			1.08	1.13	1.08	2.48	p	ADO
HIP 78530 -1	>14.50	14.56	14.22	4.54	139.69	(>8.71)	(8.77)	(8.43)	(≈0.02)	?	ADO
HIP 78809	7.41	7.50	7.51			1.65	1.74	1.75	2.03	p	ADO
HIP 78809 -1	11.08	10.45	10.26	1.18	25.67	5.32	4.69	4.50	0.30	c	ADO
HIP 78956	7.52	7.54	7.57			1.15	1.17	1.20	2.40	p	ADO
HIP 78956 -1	9.76	9.12	9.04	1.02	48.67	3.39	2.75	2.67	1.16	c	ADO
HIP 79124	7.16	7.14	7.13			1.11	1.09	1.08	2.48	p	ADO
HIP 79124 -1	11.38	10.55	10.38	1.02	96.18	5.33	4.50	4.33	0.33	c	ADO
HIP 79156	7.56	7.56	7.61			1.44	1.44	1.49	2.09	p	ADO
HIP 79156 -1	11.62	10.89	10.77	0.89	58.88	5.50	4.77	4.65	0.27	c	ADO
HIP 80238	7.45	7.45	7.34			1.83	1.83	1.72	1.94	p	ADO
HIP 80238 -1	7.96	7.66	7.49	1.03	318.46	2.34	2.04	1.87	1.67	c	ADO

Table A.2. Criteria used to determine whether a secondary is a companion star or a background star. Results are listed for secondaries found around the 22 targets observed with NACO (*top part of the table*) and the 9 targets with multi-color observations in the ADONIS dataset (*bottom part of the table*). Columns 1 and 2 show the secondary designation and the status of the component as determined in this paper (c = companion star; ? = candidate companion star; b = background star). Columns 3−5 show the compatibility of the location of the object in the color–magnitude diagrams with the isochrones in terms of χ^2. Confirmed companions have $\chi^2 < 2.30$ and (confirmed) background stars have $\chi^2 > 11.8$. The other secondaries have $2.30 < \chi^2 < 11.8$ and are labeled "candidate companion". A substantial fraction of these candidate companions may in fact be background stars. Several faint ($K_S > 14$ mag) secondaries are only detected in one filter (thus have no χ^2), and are all assumed to be background stars.

Star	Status	$\chi^2_{J-K_S,M_{K_S}}$	$\chi^2_{H-K_S,M_{K_S}}$	χ^2_{J-H,M_J}
HIP 59502 -1	c	2.11	1.09	0.19
HIP 59502 -2	b	—	75.23	—
HIP 59502 -3	b	—	—	—
HIP 60851 -1	b	7.77	1.29	15.51
HIP 60851 -2	b	>52.81	0.19	>45.54
HIP 60851 -3	?	—	7.54	—
HIP 60851 -4	b	—	22.34	—
HIP 60851 -5	b	—	26.37	—
HIP 60851 -6	b	—	—	—
HIP 60851 -7	b	—	—	—
HIP 60851 -8	b	—	237.30	—
HIP 61265 -1	?	4.46	0.02	3.83
HIP 61265 -2	b	13.77	1.81	5.29
HIP 61265 -3	b	—	13.70	—
HIP 61265 -4	b	—	66.72	—
HIP 61265 -5	b	—	—	—
HIP 62026 -1	c	0.91	0.09	0.24
HIP 63204 -1	b	71.62	9.64	17.02
HIP 63204 -2	c	1.76	0.01	1.38
HIP 67260 -1	c	0.01	0.00	0.01
HIP 67260 -2	?	—	7.20	—
HIP 67260 -3	?	1.45	3.59	5.27
HIP 67919 -1	c	0.02	0.86	0.39
HIP 68532 -1	c	0.93	1.10	0.00
HIP 68532 -2	c	1.06	0.02	1.70
HIP 69113 -1	c	1.26	0.09	0.63
HIP 69113 -2	c	0.56	0.04	1.38
HIP 73937 -1	c	—	0.01	—
HIP 73937 -2	b	—	22.37	—
HIP 78968 -1	?	3.88	1.26	0.73
HIP 79098 -1	b	8.45	14.45	39.65
HIP 79410 -1	b	21.58	23.51	19.09
HIP 79739 -1	c	0.44	0.09	0.91
HIP 79771 -1	c	1.46	0.24	0.52
HIP 79771 -2	nc	0.00	0.04	0.02
HIP 80142 -1	b	164.54	59.81	33.27
HIP 80142 -2	?	—	—	2.61
HIP 80474 -1	b	5.08	73.31	36.05
HIP 80799 -1	c	1.11	0.12	0.62
HIP 80896 -1	c	0.73	0.02	0.53
HIP 81949 -1	b	66.30	7.46	27.51
HIP 81949 -2	b	15.93	0.91	8.99
HIP 81949 -3	b	>13.09	0.02	>19.08
HIP 81949 -4	?	>3.88	5.69	>5.59
HIP 81949 -5	b	—	—	—
HIP 81949 -6	?	>9.95	0.98	>6.88
HIP 81949 -7	b	>5.16	>11.84	—
HIP 81949 -8	b	—	—	—
HIP 81949 -9	b	—	—	—
HIP 81949 -10	b	—	—	—
HIP 81949 -11	b	—	—	—
HIP 81949 -12	b	—	—	—
HIP 81972 -1	?	4.36	2.27	0.57
HIP 81972 -2	?	1.42	1.08	6.03
HIP 81972 -3	c	0.56	1.65	0.20
HIP 81972 -4	nc	0.51	0.11	0.13
HIP 81972 -5	nc	0.90	0.07	0.40
HIP 81972 -6	b	—	>16.02	—
HIP 81972 -7	b	—	—	—

Table A.2. continued.

Star	Status	$\chi^2_{J-K_S,M_{K_S}}$	$\chi^2_{H-K_S,M_{K_S}}$	χ^2_{J-H,M_J}
HIP 81972 -8	b	—	—	—
HIP 83542 -1	?	—	8.25	—
HIP 83542 -2	b	—	—	—
ADONIS targets with multi-color observations				
HIP 53701 -1	b	12.01	3.72	0.80
HIP 53701 -2	b	33.11	8.54	8.16
HIP 76071 -1	c	—	0.57	—
HIP 77911 -1	c	0.73	0.00	0.74
HIP 78530 -1	?	—	3.10	—
HIP 78809 -1	c	0.82	0.74	0.02
HIP 78956 -1	c	0.01	0.25	0.33
HIP 79124 -1	c	0.22	0.83	1.88
HIP 79156 -1	c	0.41	1.94	0.45
HIP 80238 -1	c	0.43	0.89	0.06

Table A.3. All companion stars identified in our ADONIS and NACO binarity surveys among A and late-B stars in Sco OB2 (Kouwenhoven et al. 2005, and this paper). The columns show the *Hipparcos* number of the primary star, the JHK_S magnitudes, the angular separation, the position angle, the current status of the companion, and the date of observation (dd/mm/yy). If measurements are performed in both the ADONIS and NACO surveys, the NACO data are provided. The wide companion of HIP 77315 at $\rho = 37.37''$ is HIP 77317, another member of Sco OB2. These stars are found to be a common proper motion pair (Worley & Douglass 1997), and were both observed in our ADONIS survey. The confirmed and candidate companions for which the status is determined using their JHK_S photometry, are indicated with "confirmed" and "inconclusive", respectively. The candidate companions identified by Kouwenhoven et al. (2005), for which the status is determined using the $K_S = 12$ mag criterion, and indicated with "candidate" here. Background stars are not listed here.

Host primary	J (mag)	H (mag)	K_S (mag)	ρ ($''$)	PA ($^\circ$)	Companion status	Date
HIP 50520			6.39	2.51	313.32	candidate	06/06/01
HIP 52357			11.45	10.04	72.69	candidate	06/06/01
HIP 52357			7.65	0.53	73.01	candidate	06/06/01
HIP 56993			11.88	1.68	23.07	candidate	06/06/01
HIP 58416			8.66	0.58	166.12	candidate	06/06/01
HIP 59413			8.18	3.18	99.83	candidate	06/06/01
HIP 59502	12.35	11.83	11.64	2.94	26.39	confirmed	06/04/04
HIP 60084			10.10	0.46	329.64	candidate	06/06/01
HIP 60851		13.63	13.69	8.16	231.46	inconclusive	06/04/04
HIP 61265	11.98	11.66	11.38	2.51	67.15	inconclusive	06/04/04
HIP 61639			7.06	1.87	182.40	candidate	07/06/01
HIP 61796			11.79	9.89	108.98	candidate	07/06/01
HIP 61796			11.86	12.38	136.77	candidate	07/06/01
HIP 62002			7.65	0.38	69.24	candidate	08/06/01
HIP 62026	8.08	7.90	7.86	0.23	6.34	confirmed	06/04/04
HIP 62179			7.57	0.23	282.75	candidate	08/06/01
HIP 63204	8.79	8.51	8.40	0.15	236.56	confirmed	06/04/04
HIP 64515			6.94	0.31	165.69	candidate	08/06/01
HIP 65822			11.08	1.82	303.87	candidate	08/06/01
HIP 67260		14.04	14.10	1.23	355.65	inconclusive	28/04/04
HIP 67260	15.84	14.83	14.67	2.33	77.25	inconclusive	28/04/04
HIP 67260	8.88	8.46	8.36	0.42	229.46	confirmed	28/04/04
HIP 67919	9.98	9.38	9.10	0.69	296.56	confirmed	28/04/04
HIP 68080			7.19	1.92	10.20	candidate	05/06/01
HIP 68532	10.52	9.85	9.54	3.05	288.50	confirmed	28/04/04
HIP 68532	11.38	10.94	10.63	3.18	291.92	confirmed	28/04/04
HIP 68867			11.61	2.16	284.76	candidate	08/06/01
HIP 69113	10.98	10.43	10.29	5.34	65.15	confirmed	30/04/04
HIP 69113	11.27	10.45	10.30	5.52	67.17	confirmed	30/04/04
HIP 69749			11.60	1.50	0.84	candidate	08/06/01
HIP 70998			10.83	1.17	354.60	candidate	06/06/01
HIP 71724			9.70	8.66	23.02	candidate	08/06/01
HIP 71727			7.80	9.14	244.96	candidate	08/06/01
HIP 72940			8.57	3.16	221.58	candidate	06/06/01
HIP 72984			8.50	4.71	260.35	candidate	06/06/01
HIP 73937		8.46	8.37	0.24	190.58	confirmed	30/04/04
HIP 74066			8.43	1.22	109.62	candidate	08/06/01
HIP 74479			10.83	4.65	154.15	candidate	08/06/01
HIP 75056			11.17	5.19	34.51	candidate	08/06/01
HIP 75151			8.09	5.70	120.87	candidate	08/06/01
HIP 75915			8.15	5.60	229.41	candidate	05/06/01
HIP 76001			7.80	0.25	3.17	candidate	08/06/01
HIP 76001			8.20	1.48	124.82	candidate	08/06/01
HIP 76071		11.28	10.87	0.69	40.85	confirmed	02/06/00, 07/06/01
HIP 77315			7.12	37.37	137.32	candidate	08/06/01
HIP 77315			7.92	0.68	67.01	candidate	05/06/01
HIP 77911	12.68	12.20	11.84	7.96	279.25	confirmed	02/06/00, 07/06/01
HIP 77939			8.09	0.52	119.13	candidate	31/05/00
HIP 78530		14.56	14.22	4.54	139.69	inconclusive	02/06/00, 07/06/01
HIP 78756			9.52	8.63	216.40	candidate	02/06/00
HIP 78809	11.08	10.45	10.26	1.18	25.67	confirmed	03/06/00, 07/06/01
HIP 78847			11.30	8.95	164.02	candidate	03/06/00
HIP 78853			8.45	1.99	270.39	candidate	08/06/01

Table A.3. continued.

Host primary	J (mag)	H (mag)	K_S (mag)	ρ ($''$)	PA (°)	Companion status	Date
HIP 78956	9.76	9.12	9.04	1.02	48.67	confirmed	03/06/00, 07/06/01
HIP 78968	14.96	14.51	14.26	2.78	322.13	inconclusive	04/05/04
HIP 79124	11.38	10.55	10.38	1.02	96.18	confirmed	03/06/00, 07/06/01
HIP 79156	11.62	10.89	10.77	0.89	58.88	confirmed	03/06/00, 07/06/01
HIP 79250			10.71	0.62	180.92	candidate	03/06/00
HIP 79530			8.34	1.69	219.66	candidate	31/05/00
HIP 79631			7.61	2.94	127.85	candidate	05/06/01
HIP 79739	12.28	11.52	11.23	0.96	118.33	confirmed	19/06/04
HIP 79771	12.00	11.28	10.89	3.67	313.38	confirmed	19/06/04
HIP 79771	12.39	11.79	11.42	0.44	128.59	confirmed	19/06/04
HIP 80142	16.64	15.88		5.88	119.94	inconclusive	04/05/04
HIP 80238	7.96	7.66	7.49	1.03	318.46	confirmed	02/06/00, 07/06/01
HIP 80324			7.52	6.23	152.46	candidate	31/05/00, 03/06/00
HIP 80371			8.92	2.73	140.65	candidate	02/06/00, 03/06/00
HIP 80425			8.63	0.60	155.77	candidate	08/06/01
HIP 80461			7.09	0.27	285.64	candidate	31/05/00
HIP 80799	10.60	10.04	9.80	2.94	205.02	confirmed	05/05/04
HIP 80896	11.16	10.63	10.33	2.28	177.23	confirmed	08/06/04
HIP 81624			7.95	1.13	224.28	candidate	05/06/01
HIP 81949		15.62	14.82	6.26	239.37	inconclusive	04/05/04, 05/05/04, 08/06/04, 25/06/04
HIP 81949		15.67	15.52	5.27	340.72	inconclusive	04/05/04, 05/05/04, 08/06/04, 25/06/04
HIP 81972	11.30	10.97	10.61	7.02	258.81	inconclusive	27/06/04
HIP 81972	11.63	10.87	10.48	2.02	313.69	inconclusive	27/06/04
HIP 81972	12.54	11.86	11.77	5.04	213.45	confirmed	27/06/04
HIP 81972	15.10	14.43	13.98	2.79	106.94	confirmed	27/06/04
HIP 81972	16.11	15.63	15.26	7.92	229.27	confirmed	27/06/04
HIP 83542		9.72	9.90	8.86	196.21	inconclusive	10/09/04
HIP 83693			9.26	5.82	78.35	candidate	06/06/01